Using TOPSIS to Find the Best Model to Estimate Mean Hourly Irradiation at the “Cirque de Mafate” in Reunion Island

Tovondahiniriko Fanjirindratovo[1*], Didier Calogine[2], Oanh Chau[2], Olga Ramiarinjanahary[1]

[1] Physics and Environment Laboratory, University of Toliara, Madagascar.
[2] PIMENT Laboratory, University of Reunion Island, La Réunion, France.

* Corresponding author. Email: fanjiry@gmail.com (T.F.)
Manuscript submitted December 4, 2023; revised March 3, 2024; accepted March 30, 2024; published July 31, 2024.
doi: 10.12720/sgce.13.3.65–93

Abstract: In this paper, nineteen models were used to estimate the monthly average hourly global solar irradiation from the daily global irradiation value; at the “Cirque de Mafate” which is an isolated high mountain and rugged relief site in Reunion Island. These models are divided into three groups; the first depends on solar parameters like hour angle or solar time, the second implies that the estimation function follows a Gaussian distribution, and the third is a simplified form of the first. The main target is to find, for the site, the best model to estimate the abovementioned monthly average hourly irradiation. The measured data used to validate the models are from an in situ weather station. The following statistical criteria; normalized mean bias error, normalized absolute mean bias error, normalized root mean square, t-statistical test, correlation coefficient, relative standard error and Nash-Sutcliffe Equation were used to evaluate the performance for each model. To rank and compare the nineteen models by the abovementioned seven criteria, the Multi-Criteria Decision Making (MCDM) approach has been used and especially the Technique for Order Preference by Similarity to the Ideal Solution (TOPSIS). The basic principle of TOPSIS is to define the ideal model and the worst model by the set of the statistical criteria’s value for all models. Then the Euclidian distance to the ideal model and/or the worst model is calculated. The best model is the one that is nearest the ideal model and farthest the worst model. To use the TOPSIS, a normalized weight, that indicates the importance or priority, for each statistical criterion has been calculated by objective and subjective way. As result, it was found that the best model came from the first group and it is the Collares-Pereira and Rabl model modified by Gueymard (CPRG) and in second position is the Gueymard model.

Keywords: Clearness index, mean hourly irradiation from daily value, objective and subjective weight, Technique for Order Preference by Similarity to the Ideal Solution (TOPSIS)

1. Introduction

A solar PV smart grid was installed at Roche Plate in the “Cirque de Mafate”, at Reunion Island, Indian Ocean [1]. It is an isolated area in a high mountain, with rugged relief and accessible only by foot or helicopter. An Energy Management System (EMS) was implemented in the smart grid to manage in real time the user’s needs and available solar energy resources [2–4]. So, the estimation and/or prevision of the solar irradiation are important parts of this real time EMS, especially the hourly irradiation. A meteorological station is also installed in situ to measure weather parameters and the global solar radiation on horizontal and titled plane. Seen that the PV solar smart grid is the best way to provide electricity for the population at Roche Plate, other smart grids are planned to be installed, and the experience from this first smart grid will be used to develop the others, particularly the EMS. The aim of this paper is first to study the main features of solar irradiation in a high mountain and rugged relief site like the Cirque of Mafate, and then to find, among the existing, the best model to estimate the ratio of the mean hourly and daily irradiation that is, as shown above, a key parameter for the EMS. The data collected, by in situ weather station, from March 2020 to August 2022 were used to validate the models [5]. Nineteen models from the literature have been applied, and the performance of each model was evaluated by seven statistical criteria. So to rank nineteen models by seven criteria, the Multi-Criteria Decision Making (MCDM) approach has been used especially the Technique for Order Preference by Similarity to Ideal Solution (TOPSIS). The main constraint when using MCDM approach is that a normalized weight should be assigned to the different criteria according to their relative importance between them. In this work, objective methods (entropy and CRITIC) and subjective weighting methods (Analytic Hierarchy Process) are used together. The knowledge of the principal features of solar irradiation will help in the future for the design of a new model which better corresponds to the present site. This paper will be divided into eight parts; after the introduction, the second part is for site presentation, then the third is a literature review about the hourly radiation models and the statistical criteria. The fourth part is for MCDM method by TOPSIS with the weighting. The fifth is for the final methodology for this work, followed by the results, discussion and conclusion.

2. Site Presentation and Database

Fig. 1 gives the geographical location of the site and GPS coordinates are −21.06953° S, 55.406328° E. It is an isolated area in a high mountain place, accessible only by foot or helicopter.

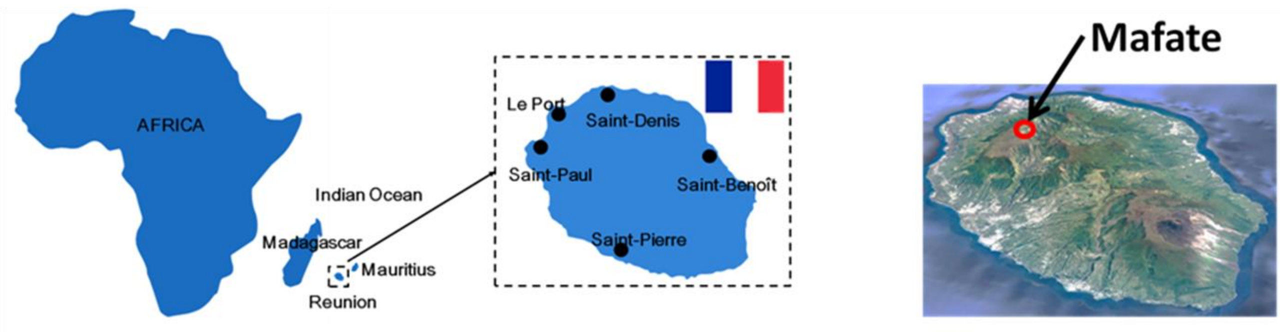

Fig. 1. Geographical location of the Roche Plate, Cirque de Mafate.

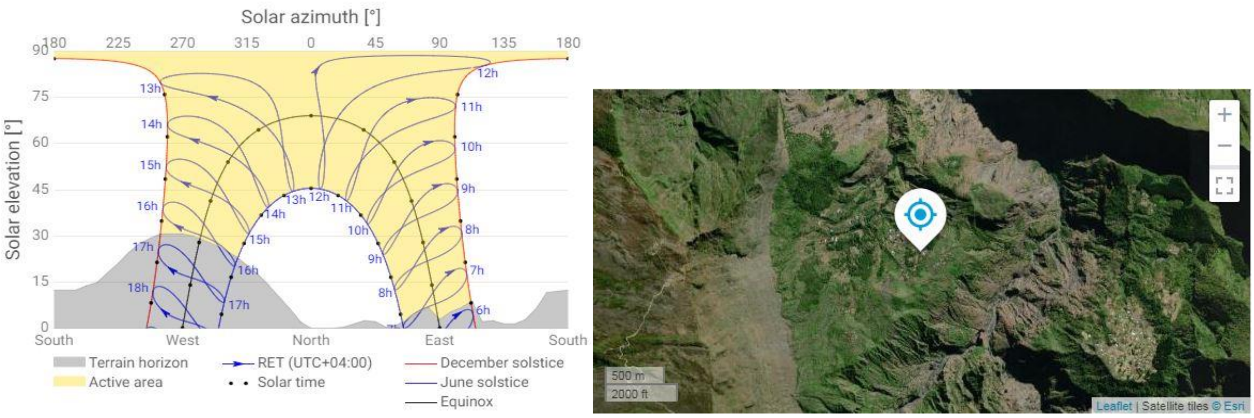

(a) (b)

Fig. 2. Topographic parameters: (a) sun path and horizon relief mask, (b) relief satellite view.

Fig. 2 shows the sun path, horizon mask and, by satellite view, the relief around. This latter is very rugged. On the west side, there is a near high mountain wall as a mask relief. Fig. 2 was extracted from the website: www.globalsolaratlas.com.

The database is obtained from in situ weather station that measures the global solar radiation G in kW/m² every 20 seconds [5]. Then the hourly irradiation I_h and the daily irradiation H_h in kWh/m² are calculated. The following main astronomical data were calculated by the Michalsky's algorithm [6]:

- solar azimuth *azs*, elevation α and declination δ angle, in degree
- hourly angle ω, sunrise ω_o and sunset ω_s angle, in degree
- sun-earth distance correction factor ε
- the hourly I_{oh} and daily H_{oh} extraterrestrial irradiation on a horizontal plane in (kWh/m²)

According to Refs. [7] and [8], the hourly data that satisfy the following criteria were selected for the study

$$0 \le I_h \le 0.9 I_{oh} \tag{1}$$

$$0 \le H_h \le 0.8 H_{oh} \tag{2}$$

and the last test in this paper is for solar elevation angle

$$\alpha > 0 \tag{3}$$

To calculate the hourly irradiation value at a given *h* hour, radiation data from *h*−30 min to *h*+30 min were used. Seen that the area is in a tropical site, the hourly data are mainly for 06:00 to 18:00. After that, the mean of hourly irradiation *I*, daily irradiation *H* and extraterrestrial irradiation H_0 in kWh/m² were calculated. These mean values can be monthly, annual, for austral winter, and austral summer.

3. Literature Review of Hourly Irradiation Models and Statistical Criteria

The goal is to estimate the ratio *r* of the mean hourly irradiation and the mean daily value of irradiation

$$r = \frac{I}{H} \tag{4}$$

The existing models can be divided into three groups; the first calculates the ratio *r* as a function of the hour angle ω or solar time t_s, and other solar parameters. The second, which is a function of the solar time t_s only, implies that the weather conditions are random and the ratio follows a Gaussian distribution. The last is a simplified form of the first, and the ratio is a function of time only and does not take into account other solar parameters nor the randomness of solar radiation. Table 1 gives the models on the first group. Tables 2 and 3 are respectively for second and third group.

For the first group, the first model is the Whillier [9] model which was simplified by the Liu and Jordan [10] model. This latter whose notation is r_0 in Table 1 is the base of all other models except the Kaplanis model. Then Garg & Garg model [11] and Collares-Pereira and Rabl (CPR) model were built based on Liu and Jordan [10] model r_0. Gueymard improved the CPR model to get the Collares-Pereira and Rabl modified by Gueymard model (CPRG). After that, Gueymard built also his own model, always based on r_0. The last model is the Kaplanis model which does not depend on r_0.

For the second group in Table 2, the ratio fits a Gaussian curve and the variable is the true solar time t_s. The standard deviation is

$$\sigma = \frac{1}{r_{12}\sqrt{2\pi}} \tag{5}$$

$$r_{12} = \frac{I(t_s = 12)}{H} \tag{6}$$

r_{12} is the ratio of the hourly and the daily irradiation at noon solar time. The first model was Jain 1 that was improved by Baig 1, and this latter was improved also by Shazly 1. If r_{12} is unknown, the standard deviation is related to the day length S. Jain, Baig and Shazly proposed formulas for their models, to get σ from S (Jain 2, Jain 3, Baig 2, Shazly 2). Then Kaplanis also, proposed two formulas to get σ from S for Jain and Baig model based on the Gaussian distribution characteristics (Jain 4, Jain 5, Baig 3, Baig 4).

Table 1. The First Group's Models

Model	Formula	Reference
Whillier	$r_W = \frac{\pi}{24} \cdot \frac{\frac{24}{\pi}\sin\frac{\pi}{24}\cos\omega - \cos\omega_s}{\sin\omega_s - \left(\frac{\pi\omega_s}{180}\cos\omega_s\right)}$	[9]
Liu & Jordan	$r_{L\&J} = r_0 = \frac{\pi}{24} \cdot \frac{\cos\omega - \cos\omega_s}{\sin\omega_s - \left(\frac{\pi\omega_s}{180}\cos\omega_s\right)}$	[10]
Garg & Garg	$r_{G\&G} = r_0 - 0.008\sin 3\left(\frac{\pi\omega_s}{180} - 0.65\right)$	[11]
CPR	$r_{CPR} = (a + b\cos\omega)\, r_0$ $a = 0.4090 + 0.5016\sin(\omega_s - 60°)$ $b = 0.6609 - 0.4767\sin(\omega_s - 60°)$	[12]
CPRG	$r_{CPRG} = (a + b\cos\omega) r_0 / f$ $f = a + 0.5b \frac{\frac{\pi\omega_s}{180} - \sin\omega\cos\omega_s}{\sin\omega_s - \left(\frac{\pi\omega_s}{180}\cos\omega_s\right)}$	[13]
Gueymard	$r_G = r_0 \frac{1 + q\frac{a_2}{a_1}k.A(\omega_S) r_0}{1 + q\frac{a_2}{a_1}.\frac{A(\omega_S)}{B(\omega_S)}}$ $k = 24/\pi$ and $q = \cos\Phi\cos\delta$ Φ : site's latitude $A(\omega_S) = \sin\omega_s - \frac{\pi\omega_s}{180}\cos\omega_s$ $B(\omega_S) = \frac{\pi\omega_s}{180}\left(0.5 + \cos^2\omega_s\right) - 0.75\sin(2\omega_s)$ $a_1 = 0.41341K_t + 0.61197K_t^2 - 0.01886K_t.S + 0.00759.S$ $a_2 = \max\left(0.054, 0.28116 + 2.2475K_t - 1.76118K_t^2 - 1.84535\sin h_0 + 1.6811\sin^3 h_0\right)$ $K_t = \frac{H}{H_0}$, then $S = 2\frac{\omega_s}{15}$ and $\sin h_0 = qA(\omega_S)/\left(\frac{\pi\omega_s}{180}\right)$	[14]
Kaplanis	$r_K = \frac{\alpha + \beta\cos(2\pi.t_s/24)}{2\alpha(t_{ss} - 12) + (24\beta/\pi)\sin(2\pi.t_{ss}/24)}$ t_{ss}, is the sunset solar time, the equations to get α and β are $\begin{cases} 2\alpha(t_{ss} - 12) + (24\beta/\pi)\sin(2\pi.t_{ss}/24) = H \\ \alpha + \beta\cos(2\pi.t_s/24) = 0 \end{cases}$ H is the irradiation for the day	[15]

Table 2. The Second Group's Models

Model	Formula	Reference
Jain 1	$r_{j1}=\frac{1}{\sigma\sqrt{2\pi}}\exp\left(-\frac{(t_s-12)^2}{2\sigma^2}\right)$	[16]
Jain 2	$r_{j2}=\frac{1}{\sigma_2\sqrt{2\pi}}\exp\left(-\frac{(t_s-12)^2}{2\sigma_2^2}\right)$ $\sigma_2=0.192S+0.461$	[16]
Jain 3	$r_{j3}=\frac{1}{\sigma_3\sqrt{2\pi}}\exp\left(-\frac{(t_s-12)^2}{2\sigma_3^2}\right)$ $\sigma_3=0.2S+0.378$	[17]
Jain 4	$r_{j4}=\frac{1}{\sigma_4\sqrt{2\pi}}\exp\left(-\frac{(t_s-12)^2}{2\sigma_4^2}\right)$ $\sigma_4=0.25S$	[15]
Jain 5	$r_{j5}=\frac{1}{\sigma_5\sqrt{2\pi}}\exp\left(-\frac{(t_s-12)^2}{2\sigma_5^2}\right)$ $\sigma_5=0.246S$	[15]
Baig 1	$r_{B1}=\frac{1}{\sigma\sqrt{2\pi}}\left(\exp\left(-\frac{(t_s-12)^2}{2\sigma^2}\right)+\cos\left(180\frac{t_s-12}{S-1}\right)\right)$	[18]
Baig 2	$r_{B2}=\frac{1}{\sigma_6\sqrt{2\pi}}\left(\exp\left(-\frac{(t_s-12)^2}{2\sigma_6^2}\right)+\cos\left(180\frac{t_s-12}{S-1}\right)\right)$ $\sigma_6=0.21S+0.26$	[18]
Baig 3	$r_{B3}=\frac{1}{\sigma_4\sqrt{2\pi}}\left(\exp\left(-\frac{(t_s-12)^2}{2\sigma_4^2}\right)+\cos\left(180\frac{t_s-12}{S-1}\right)\right)$	[15]
Baig 4	$r_{B4}=\frac{1}{\sigma_5\sqrt{2\pi}}\left(\exp\left(-\frac{(t_s-12)^2}{2\sigma_5^2}\right)+\cos\left(180\frac{t_s-12}{S-1}\right)\right)$	[15]
Shazly 1	$r_{S1}=\frac{1}{2.2\sigma\sqrt{2\pi}}\left(\exp\left(-\frac{(t_s-12)^2}{2\sigma^2}\right)+1.2\cos\left(180\frac{t_s-12}{S-1}\right)\right)$	[19]
Shazly 2	$r_{S2}=\frac{1}{2.2\sigma_7\sqrt{2\pi}}\left(\exp\left(-\frac{(t_s-12)^2}{2\sigma_7^2}\right)+1.2\cos\left(180\frac{t_s-12}{S-1}\right)\right)$ $\sigma_7=0.174S+0.768$	[19]

And in the third group, there is only one model that is the Newell model as seen in Table 3.

Table 3. The Third Group's Model

Model	Formula	Reference
Newell	$r_N=\frac{1.5}{S}\left(1-\frac{4(t_s-12)^2}{S}\right)$	[20]

Table 4 gives the statistical criteria commonly used in the literature [7, 21, 22].

ms_i is the *i-th* measured value, ms_a is the average value of all ms_i.

c_i is the *i-th* calculated value, c_a is the average value of all c_i.

n_o is the number of measurement points.

An important aspect is to define for each criterion the best value, i.e. the value towards which the criterion must tend for the best model according to this criterion. If the best value is 1 or the highest as possible, the criterion is called a benefit criterion. If the best value is 0 or the lowest as possible, the criterion is called a cost criterion.

Table 4. The Statistical Analysis Crteria

Criterion	Formula	Best value
Nash-Sutcliffe Equation NSE	$NSE = 1 - \frac{\sum_{i=1}^{i=n_0}(ms_i - c_i)^2}{\sum_{i=1}^{i=n_0}(ms_i - ms_a)^2}$	1
Correlation coefficient R	$R = \frac{\sum_{i=1}^{i=n_0}(c_i - c_a)(ms_i - ms_a)}{\sqrt{\left(\sum_{i=1}^{i=n_0}(c_i - c_a)^2\right)\left(\sum_{i=1}^{i=n_0}(ms_i - ms_a)^2\right)}}$	1
Relative Standard Error (RSE)	$RSE = \sqrt{\frac{\sum_{i=1}^{i=n_0}\left(\frac{c_i - ms_i}{ms_i}\right)^2}{n_0}}$	0
Mean Bias Error (MBE)	$MBE = \frac{1}{n_0}\sum_{i=1}^{i=n_0}(c_i - ms_i)$	0
Normalized Mean Bias Error (NMBE%)	$NMBE\ \% = 100\frac{MBE}{m_a}$	0
Mean Absolute Bias Error (MABE)	$MABE = \frac{1}{n_0}\sum_{i=1}^{i=n_0}\lvert c_i - ms_i\rvert$	0
Normalized Mean Absolute Bias Error (NMABE%)	$NMABE\ \% = 100\frac{MABE}{m_a}$	0
Root Mean Square Error (RMSE)	$RMSE = \sqrt{\frac{1}{n_0}\sum_{i=1}^{i=n_0}(c_i - ms_i)^2}$	0
Normalized Root Mean Square Error (NRMSE%)	$NRMSE\ \% = 100\frac{RMSE}{m_a}$	0
t-stat	$t - stat = \sqrt{\frac{(n_0 - 1)MBE^2}{RMSE^2 - MBE^2}}$	0

4. The MCDM Method by TOPSIS

The Multi-Criteria Decision Making (MCDM) is a method to rank *m* models by *n* criteria. There are several MCDM methods and the one that is used here is the Technique for Order Preference by Similarity to Ideal Solution or TOPSIS [23–25]. The goal of the TOPSIS is to identify the ideal model called here Positive Ideal Model and the opposite that is the worst model called the Negative Ideal Model. Then, the Euclidian distance between the PIM and NIM is calculated for each model. The best model is the one that is nearest the PIM and farthest the NIM. The different steps in TOPSIS are like the following.

4.1. Steps for TOPSIS procedure

a) Build the (*m*,*n*) decision matrix $dm_{(m*n)}$ with *m* rows for the models or methods, and *n* columns for the criteria. So $dm_{(i,j)}$ represents the value of the j^{th} criterion for the i^{th} model

$$dm = \left.\overbrace{\begin{pmatrix} dm_{11} & dm_{12} & \dots & \dots & dm_{1n} \\ dm_{21} & dm_{22} & \dots & \dots & dm_{2n} \\ \dots & \dots & \dots & \dots & \dots \\ \dots & \dots & \dots & \dots & \dots \\ dm_{m1} & dm_{m2} & \dots & \dots & dm_{mn} \end{pmatrix}}^{n\ criteria}\right\} m\ methods \tag{7}$$

b) Normalize the *dm* matrix to obtain *r* matrix as

$$r_{ij} = \frac{dm_{ij}}{\sqrt{\sum_{i=1}^{i=m} dm_{ij}^2}} \tag{8}$$

c) Build the vector *w* containing the weight of each criterion

$$w = (w_1, w_2, \dots, w_n),\quad w_j > 0 \text{ and } \sum_{i=1}^{i=m} w_j = 1 \tag{9}$$

The weighting method will be fully explained on the next paragraph

d) Compute the weighted normalized decision matrix *v*

$$v_{ij} = w_j \times r_{ij} \text{ for } i=1,2,\dots,m \text{ and } j=1,2,\dots,n \tag{10}$$

e) For each column of *v* find the best and the worst value according to the criterion. The best values will be the component of the PIM and the worst values the component of NIM.

$$PIM = (v_1^+, v_2^+, \dots, v_n^+) \text{ and } NIM = (v_1^-, v_2^-, \dots, v_n^-) \tag{11}$$

If the *j-th* criterion is a benefit criterion

$$v_j^+ = \max_i v_{ij} \text{ and } v_j^- = \min_i v_{ij} \tag{12a}$$

Otherwise, if the *j-th* criterion is a cost criterion

$$v_j^+ = \min_i v_{ij} \text{ and } v_j^- = \max_i v_{ij} \tag{12b}$$

f) From each model compute the Euclidian distance from PIM (D^+) and NIM (D^-).

$$D_i^+ = \sqrt{\sum_{j=1}^{n_0} (v_{ij} - v_j^+)^2} \text{ and } D_i^- = \sqrt{\sum_{j=1}^{n_0} (v_{ij} - v_j^-)^2} \tag{13}$$

g) Then the model's relative closeness to the NIM and PIM is

$$rcn_i = \frac{D_i^-}{D_i^+ + D_i^-} \text{ and } rcp_i = \frac{D_i^+}{D_i^+ + D_i^-} \tag{14}$$

h) Finally, the ranking from best to worst is in decreasing order if *rcn* is used (the best is the farthest NIM), or in increasing order if *rcp* is used (the best is nearest PIM).

4.2. Weighting methods

An important part of the MCDM is the weighting method where some coefficients of importance are given for each criterion. The weights are normalized, so their sum for all the criteria is 1 according to relation Eq. (9). There are two basic methods, the subjective and the objective. For the subjective one, the weighting depends on the experience and human decision. For objective method, the weight depends only on the numerical data in the decision matrix. On this study, these two methods are used and combined together.

For the subjective method, the simplest way is the Rank Sum or Rank Exponent method [26], when the decision maker gives a hierarchy or sorts by high importance to low the criteria, then the rank of each criterion is converted to a normalized weight. But the subjective method that allows more analyze between criteria is the Analytic Hierarchy Process (AHP).

For the objective method, the weight of each criterion depends on the dispersion of the model's value for this criterion. If for a criterion, the values from the different models are much closer together, there is a little information to differentiate the models, so the weight of this criterion is lower. And in the opposite, if the dispersion value for the criterion is high, the models are sufficiently spaced apart from each other, so there is enough information to differentiate them, and the weight for this criterion is higher. The first basic objective methods are the standard deviation and variance method, where the normalized weight is equal to the standard deviation or variance value for the criterion divided by the sum of all standard deviation or variance of all criteria [26]. The usual objective methods are the entropy method to evaluate the diversity of information inside the data set, and the CRiteria Importance Through Inter-Criteria (CRITIC) method, that also analyses the correlation between criteria, through the dispersion.

4.3. The Analytic Hierarchy Process (AHP)

The decision maker compares criteria in pairs, to determine whether they are significantly different from one another [26, 27]. This comparison gives a $M_{(n*n)}$ matrix called judgment matrix as shown in the Table 5 for an example with five criteria.

Table 5. Example of Judgment Matrix for Five Criteria

	c_1	**c_2**	**c_3**	**c_4**	**c_5**
c_1	**1**	1/3	1/9	1/5	1/4
c_2	3	**1**	1	1	1
c_3	9	1	**1**	3	1
c_4	5	1	1/3	**1**	2
c_5	4	1	1	1/2	**1**

M_{ij} is the comparison between criteria c_i and c_j. If criterion c_i has more importance than criterion c_j, an integer number called intensity value, between 1 to 9 is given to M_{ij} . The diagonal of the judgment matrix is always 1, and

$$M_{ij} = \frac{1}{M_{ji}} \tag{15}$$

On the example above, the criterion c_1 has the lowest importance than other criteria. Criterion c_3 is more important than c_4. Criterion c_4 is more important than c_5, and c_3 has an equal importance to c_5. Criterion c_2 has an equal importance to c_3, c_4, and c_5. For the j^{th} criterion the normalized weight is

$$w_j = \frac{\left(\prod_{k=1}^{k=n} M_{jk}\right)^{1/n}}{\sum_{l=1}^{l=n}\left(\prod_{k=1}^{k=n} M_{lk}\right)^{1/n}} \tag{16}$$

To validate the result, a parameter named Consistency Ratio (CR) should be calculated and its value should be lower than 0.1. To compute CR, the following step should be followed.

Compute the n dimensional vector λ

$$\lambda_i = \frac{1}{w_i}\sum_{j=1}^{j=n} M_{ij}.w_j \tag{17}$$

If the mean value of λ is inferior to n, there are errors in the previous calculation. If not, another parameter called Consistency Index (CI) is calculated by

$$CI = \frac{mean(\lambda) - n}{n-1} \tag{18}$$

Then, the Random Index (RI) parameter is found inside the Table 6 below.

Table 6. Random Index Table

n	RI
1	0.00
2	0.00
3	0.58
4	0.90
5	1.12
6	1.24
7	1.32
8	1.41
9	1.45
10	1.49
11	1.51
12	1.54
13	1.56
14	1.57
15	1.59

Finally, the consistency ration CR is given by

$$CR = \frac{CI}{RI} \tag{19}$$

If CR < 0.1, the result is acceptable, otherwise the judgment matrix should be revisited.

4.4. The objective entropy weighting

The start is again the decision matrix $dm_{(m\times n)}$ with m rows for the models and n columns for the criteria, the normalized matrix p is [25, 27, 28]:

$$p_{ij} = \frac{dm_{ij}}{\sum_{i=1}^{i=m} dm_{ij}}, \quad i=1,2,..,m \quad \text{and} \quad j=1,2,..,n \tag{20}$$

The entropy information of the j^{th} criterion is

$$e_j = -\frac{1}{\ln(m)} \sum_{i=1}^{i=m} p_{ij}.\ln(p_{ij}) \tag{21}$$

The degree of diversity of the information involved in the j^{th} criterion is

$$d_j = 1 - e_j \tag{22}$$

And the weight for the j^{th} criterion is

$$w_j = \frac{d_j}{\sum_{k=1}^{k=n} d_k} \tag{23}$$

4.5. The Criteria Importance Through Inter-Criteria (CRITIC) method

This method, takes also into account the correlation between criteria. First, the decision matrix is normalized to get the ρ matrix [26, 29].

$$\rho_{ij} = \frac{dm_{ij} - dm_{j\min}}{dm_{j\max} - dm_{j\min}} \tag{24}$$

for benefit criteria and

$$\rho_{ij} = \frac{dm_{j\max} - dm_{ij}}{dm_{j\max} - dm_{j\min}} \tag{25}$$

for cost criteria

$dm_{j\max}$, is the highest value for the j^{th} criterion, and $dm_{j\min}$ is the lowest value.

The correlation matrix *cr* (that is an *n* square matrix) between criteria is:

$$cr_{jk} = \frac{\sum_{i=1}^{i=m}\left(\rho_{ij} - \overline{\rho_j}\right)\left(\rho_{ik} - \overline{\rho_k}\right)}{\sqrt{\sum_{i=1}^{i=m}\left(\rho_{ij} - \overline{\rho_j}\right)^2\left(\rho_{ik} - \overline{\rho_k}\right)^2}} \quad j,k=1,2,..,n \tag{26}$$

with $\overline{\rho_j}$ the mean value of the j^{th} column

The weight per criterion is

$$w_j = \frac{\sigma_j \sum_{k=1}^{k=n}\left(1 - cr_{jk}\right)}{\sum_{l=1}^{l=n}\left(\sigma_l \sum_{k=1}^{k=n}\left(1 - cr_{lk}\right)\right)} \tag{27}$$

where σ_j is the standard deviation of the j^{th} criterion.

4.6. Combination of objective and subjective weight

Subjective and objective weighting have their advantages and inconveniences. They should be combined in order to get a weight that reflects the subjective and objective behavior [30–32]. The objective weight also can be the fusion of two objective weights like CRITIC and entropy, to take into account the data dispersion and correlation between criteria.

If w_{ej} and w_{crj} represent respectively the entropy and CRITIC weight for the *j-th* criterion, the objective weight w_{oj} for this criterion is:

$$w_{oj} = \frac{w_{ej} . w_{crj}}{\sum_{j=1}^{j=n} w_{ej} . w_{crj}} \tag{28}$$

Then, if w_{sj} is the subjective weight, the combination of subjective and objective weighting is to find *a* and *b* numbers to minimize

$$\min \sum_{j=1}^{j=n}\left(a.w_{oj} - b.w_{sj}\right)^2 \tag{29a}$$

with the constraints, a+b =1, and a > 0, b > 0 (29b)

Then, the final objective and subjective combined weight will be

$$w_j = a \cdot w_{oj} + b \cdot w_{sj} \tag{30}$$

5. The Methodology of the Present Study

The proposed method in this study can be summarized as follows:

a) From the data base, the hourly (from 06:00 to 18:00) irradiation and daily irradiation for each day were calculated. Only the data that satisfy relations Eqs. (1), (2), and (3) will be retained for the study.

b) Then the averaged value of hourly irradiation (from 06:00 to 18:00) and daily irradiation were calculated for fifteen averaging periods; the twelve months of the year, the austral summer season (November to April), the austral winter season (May to October) and finally the annual averaging.

c) Apply the nineteen models for the fifteen averaging period to get the calculated data.

d) In order to use normalized value as possible, the seven following criteria were chosen and calculated: NMBE%, NMABE%, NSE, R, RSE, NRMSE% and t-stat.

e) Compute the subjective weight by AHP method. According to the study of the hourly irradiation based on daily value for Jiading Campus of Tongji University China detailed in [8], the following hierarchy respectively from high to low was used: NSE, R, RSE, MBE, MABE, RMSE and t-stat at last. But in [8] there was neither calculation of criteria's weight nor use of TOPSIS method. Wan Nik *et al.* [33] did the same study for three sites in Malaysia with MABE, MBE, RMSE and t-stat as criteria but without specifying any importance between criteria. Similar work was done also as detailed on Ref. [34] for Çanakkale in Türkiye with only NMBE%, NRMSE%, R and t-stat as criteria but without weighting or any other MCDM method.

So, for the present work, based on [8], the hierarchy in descending order is like the following; in first position from high to low are NSE, R, and RSE. In middle position there are NMBE%, NMABE%, NRMSE%, and t-stat at the end. For middle position, NMABE% and NRMSE% have equal importance. The status of NMBE% in front of the couple (NMABE% and NRMSE%) will depend later on the results data. At this stage the initial judgment matrix will be like in Table 7.

f) Compute the objective weight by the algorithm in Fig. 3.

g) With the subjective and objective weight, compute the final weight with the algorithm in Fig. 3.

h) Apply the TOPSIS method, and then by relative closeness to the NIM, rank in descending order the nineteen models for the fifteen periods. The Fig. 3 below shows the summary of algorithm to compute the final weight of each criterion.

Table 7. Initial judgment matrix

	NSE	R	RSE	NMBE%	NMABE%	NRMSE%	t-stat
NSE	1	2	3	3	3	3	5
R	1/2	1	2	3	3	3	5
RSE	1/3	1/2	1	2	3	3	5
NMBE%	1/3	1/3	1/2	1	X	X	5
NMABE%	1/3	1/3	1/3	X	1	1	5
NRMSE%	1/3	1/3	1/3	X	1	1	5
t-stat	1/5	1/5	1/5	1/5	1/5	1/5	1

X will be filled with proper value after the results of data analyze.

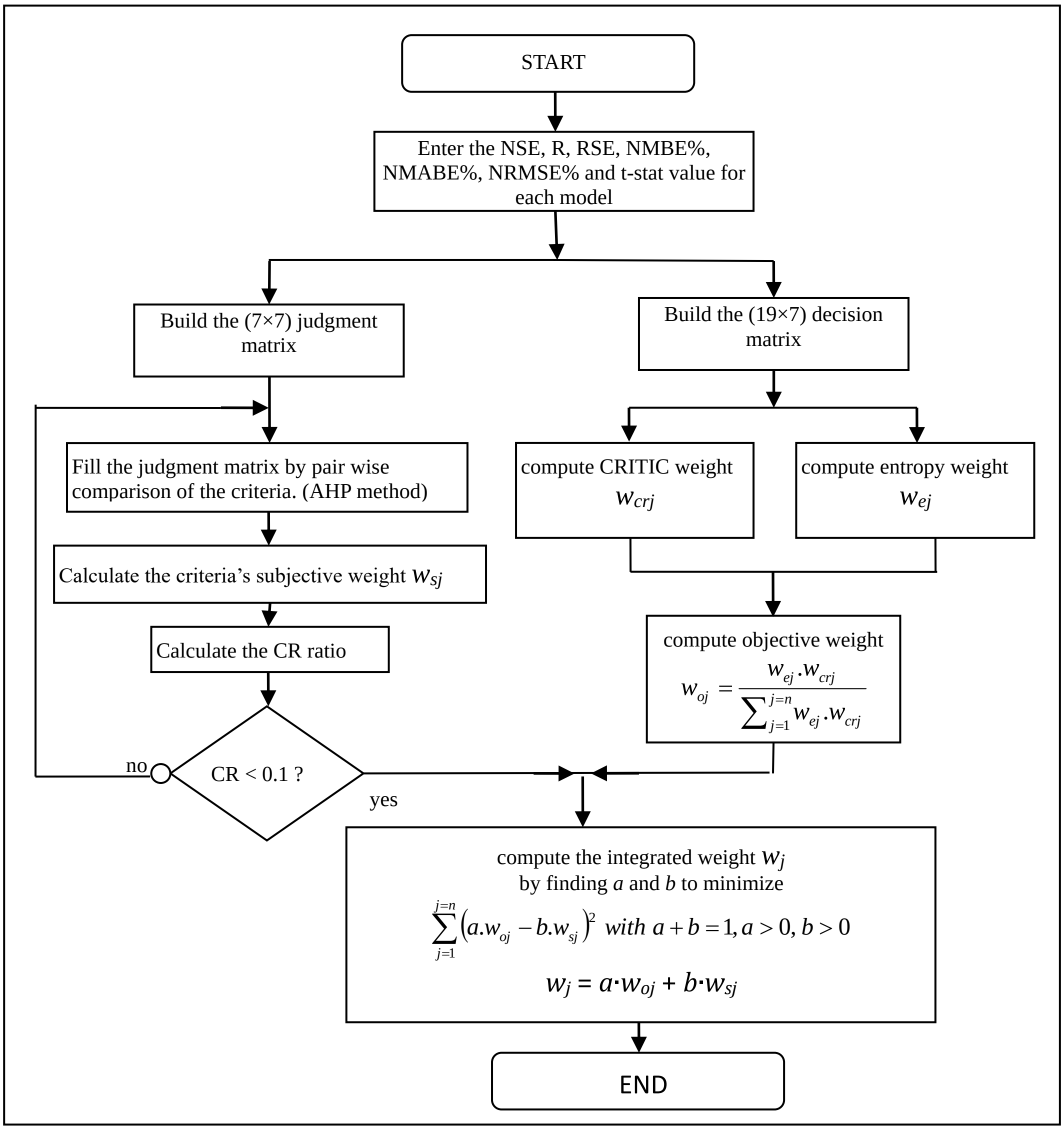

Fig. 3. Algorithm to compute integrated weight (subjective and objective).

6. Results

6.1. Plot of the measured and calculated irradiation values

In order to avoid visual confusion, only some representative models are plotted. Fig.4. gives the plot for the annual average

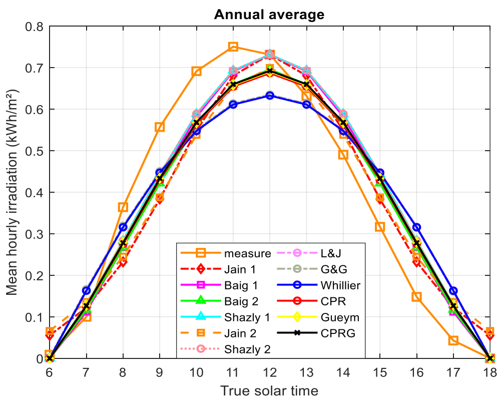

Fig. 4. Hourly measured and calculated values for a representative day of the year.

Theoretically, for a clear sky day, the irradiation curve versus time should be bell-shaped with symmetry on the morning and afternoon with respect to noon solar time, and of course the maximum is also at noon solar time, when the sun is at its highest elevation. For the present results, for the annual average, by the Fig. 4, the curve of the measured values is bell-shaped as expected, but there is no symmetry between morning and afternoon with respect to noon solar time. The maximum is at 11 h solar time. This shift of the maximum (from noon solar time to 11 h solar time) makes that for all models; there are underestimation in the morning and overestimation in the afternoon. Fig. 5 is for the month of June and the winter season average.

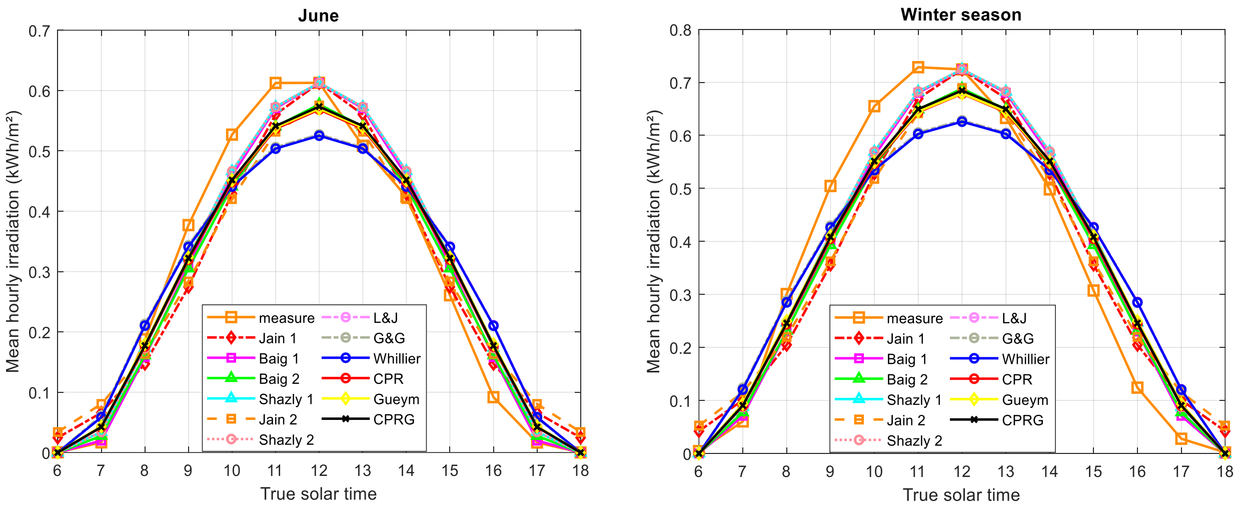

(a) (b)

Fig. 5. Measured and calculated hourly mean irradiation: (a) month of June, (b) winter season.

For the month of June and winter season averaging, even the asymmetry between morning and afternoon is still there, it is more reduced than for the annual average. The maximum is still at 11 h solar time, but practically one can assume that the maximum value holds from 11 h to noon solar time. Fig. 6 shows the same kind of plot for the month on November and the austral summer season

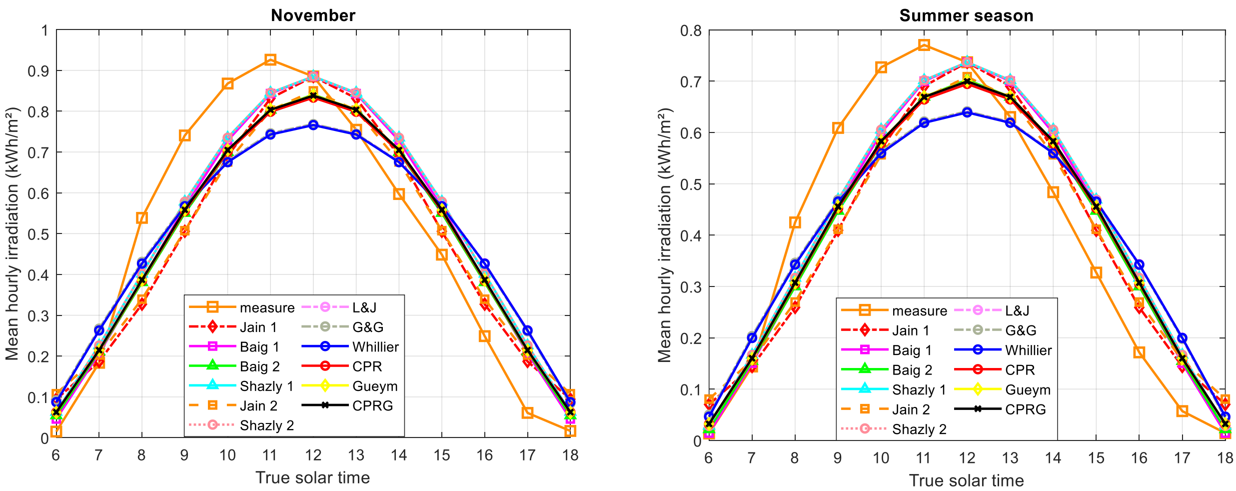

(a) (b)

Fig. 6. Measured and calculated hourly mean irradiation: (a) month of November, (b) summer season.

By Fig. 6, for the month of November and the austral summer season, the asymmetry between morning and afternoon with respect to noon solar time, for the measured value, is emphasized with the maximum always at 11 h solar time. For all models and all months there is underestimation on the morning and overestimation on the afternoon.

6.2. Plot of the hourly clearness index

The clearness index k_t is the ratio of the hourly irradiation and the extraterrestrial hourly irradiation. It can be used as indicator of the cloud coverage and the maximal value is 1.

- If k_t >0.6, it is a clear sky
- If $0.3 < k_t \leq 0.6$ it is a partly cloudy sky
- if $0 \leq k_t \leq 0.3$ it is an overcast sky

Fig. 7 gives the plot, for annual average, of k_t and Fig. 8 for austral summer and winter season. On the plot, red markers are for time before noon solar time, blue markers for afternoon and black marker for noon solar time.

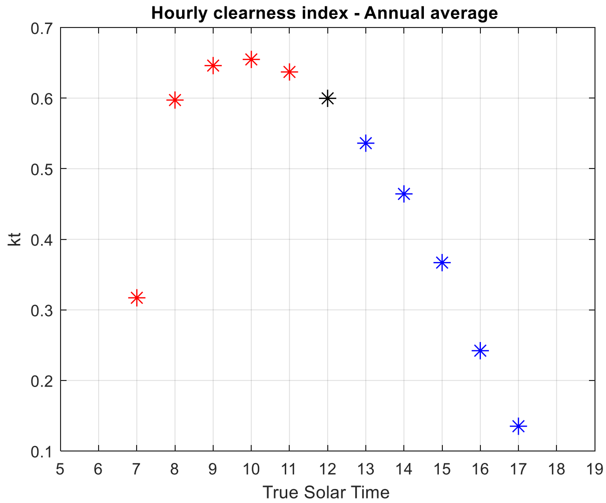

Fig. 7. The hourly clearness index for the representative day of the year.

So for the annual averaging, on the morning, it is a clear sky from 8h to noon with the maximum at 10 h. Since 11 h k_t is decreasing, and the afternoon becomes cloudier and cloudier. From 16 h, $k_t<0.3$, but it is not only from the cloud, but also from the relief mask on the west side which obscures the direct solar beam radiation from 16 h around, as it can be deduced from Fig. 2.

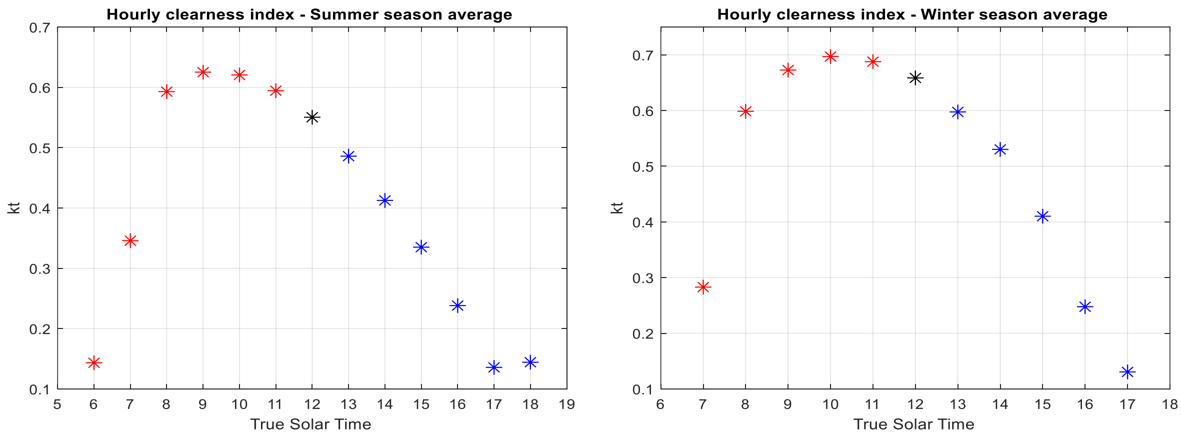

(a) (b)

Fig. 8. The hourly clearness index: (a) summer season, (b) winter season.

The behavior of the curve for winter and summer season is the same as for the annual averaging. For the summer, the clear sky is between 8 h and 11 h, with the maximum at 9h. From 10 h, k_t starts to decrease because of rising of cloud coverage as time passes. At noon solar time, it is already a partly cloudy sky. Around 16 h the effect of the cloud coverage is combined with the effect of the relief mask. For winter season, there is a clear sky in the morning until 13 h, with maximum at 10 h. Then from 11 h, the cloud coverage starts to decrease the clearness index, and in the afternoon, the effect of the relief mask overlaps on the cloud cover.

6.3. For the statistical indicators

Due to lack of room and not to make the reading cumbersome, only the tables showing the result for annual average, winter, and summer season will be shown in Tables 8, 9, and 10. For the twelve months, the results are given inside figures.

Table 8. Model's Statistical Indicators for Annual Average

year	NSE	R	RSE	NMBE(%]	NMABE(%)	NRMSE(%)	t-stat
Whillier	0.806	0.937	0.946	−0.465	22.77	24.92	0.059
Liu&Jordan	0.807	0.937	0.950	−0.179	22.68	24.85	0.023
CPR	0.861	0.938	0.663	−0.829	19.25	21.08	0.124
CPRG	0.863	0.938	0.672	0.006	19.18	20.92	0.001
G&G	0.811	0.939	0.936	−0.079	22.48	24.61	0.010
Gueymard	0.862	0.938	0.682	−0.000	19.28	21.02	0.000
Jain1	0.857	0.929	0.611	−3.259	18.17	21.37	0.488
Jain2	0.847	0.932	0.712	−4.169	19.42	22.13	0.607
Jain3	0.845	0.932	0.723	−4.271	19.54	22.25	0.618
Jain4	0.803	0.935	0.894	−6.164	22.46	25.09	0.801
Jain5	0.812	0.934	0.865	−5.805	21.82	24.49	0.771
Baig1	0.875	0.937	0.572	1.557	17.77	20.03	0.247
Baig2	0.865	0.938	0.604	−1.550	18.73	20.75	0.237
Baig3	0.829	0.938	0.655	−6.193	20.84	23.40	0.868
Baig4	0.837	0.938	0.646	−5.380	20.28	22.83	0.767
Shazly1	0.868	0.938	0.691	3.767	18.46	20.53	0.590
Shazly2	0.852	0.938	0.723	−1.427	19.81	21.76	0.208
Newell	0.761	0.934	1.108	−0.293	25.11	27.65	0.034
Kaplanis	0.807	0.937	0.950	−0.179	22.68	24.85	0.023

Table 9. Model's Statistical Indicators for Winter Season

winter	NSE	R	RSE	NMBE(%]	NMABE(%)	NRMSE(%)	t-stat
Whillier	0.856	0.958	1.129	0.001	20.55	23.08	0.000
Liu & Jordan	0.857	0.958	1.135	0.33	20.44	23.00	0.045
CPR	0.907	0.962	0.759	−0.61	16.73	18.55	0.105
CPRG	0.909	0.962	0.770	0.28	16.63	18.35	0.048
G & G	0.859	0.960	1.117	0.43	20.24	22.79	0.059
Gueymard	0.905	0.962	0.804	0.28	16.88	18.68	0.048
Jain 1	0.901	0.953	0.851	−2.65	16.20	19.07	0.444
Jain 2	0.889	0.956	1.025	−3.51	17.62	20.25	0.557
Jain 3	0.888	0.956	1.036	−3.57	17.70	20.36	0.564
Jain 4	0.850	0.959	1.278	−5.06	20.92	23.49	0.698
Jain 5	0.859	0.958	1.232	−4.75	20.25	22.80	0.674
Baig 1	0.921	0.961	0.556	1.07	14.90	17.04	0.199
Baig 2	0.912	0.961	0.621	−1.99	15.98	18.01	0.352
Baig 3	0.880	0.962	0.717	−6.16	18.53	21.02	0.970
Baig 4	0.888	0.962	0.699	−5.38	17.93	20.34	0.868
Shazly 1	0.916	0.961	0.741	3.53	15.63	17.62	0.647
Shazly 2	0.896	0.962	0.827	−2.18	17.50	19.63	0.353
Newell	0.819	0.954	1.327	0.35	22.77	25.86	0.043
Kaplanis	0.857	0.958	1.135	0.33	20.44	23.00	0.045

Table 10. Model's Statistical Indicators for Summer Season

summer	NSE	R	RSE	NMBE(%)	NMABE(%)	NRMSE(%)	t-stat
Whillier	0.832	0.932	1.191	−0.10	25.47	28.90	0.012
Liu&Jordan	0.833	0.932	1.192	0.15	25.39	28.83	0.018
CPR	0.871	0.939	0.761	−0.61	21.80	25.33	0.084
CPRG	0.872	0.939	0.770	0.10	21.75	25.20	0.014
G&G	0.836	0.934	1.203	0.27	25.20	28.55	0.033
Gueymard	0.873	0.939	0.765	0.10	21.71	25.17	0.014
Jain1	0.862	0.932	1.648	−1.80	21.89	26.22	0.238
Jain2	0.854	0.934	1.942	−2.29	23.33	26.95	0.296
Jain3	0.852	0.935	1.989	−2.38	23.55	27.12	0.305
Jain4	0.815	0.938	2.641	−3.78	27.06	30.38	0.434
Jain5	0.822	0.937	2.536	−3.52	26.30	29.75	0.413
Baig1	0.880	0.939	0.531	1.45	19.95	24.48	0.206
Baig2	0.874	0.939	0.586	−1.30	21.06	25.09	0.180
Baig3	0.845	0.938	0.805	−5.84	23.24	27.77	0.745
Baig4	0.851	0.938	0.762	−5.09	22.64	27.21	0.660
Shazly1	0.875	0.939	0.731	3.98	21.13	24.93	0.560
Shazly2	0.866	0.938	0.888	−0.25	22.50	25.83	0.034
Newell	0.797	0.923	1.465	0.18	28.36	31.80	0.020
Kaplanis	0.833	0.932	1.192	0.15	25.39	28.83	0.018

For twelve degrees of freedom, the t-stat value should be lower than 2.7188 at 95% level of confidence to validate the model. This condition is satisfied for all models and for all averaging period including each individual month.

Fig. 9, at the left, shows the plot of the NMBE% per month. The best models are those which NMBE% value tends to zero or the point per point curve is getting closer to the horizontal axis (NMBE% = 0). The models from the first group are those which curve is near the horizontal axis and their curves have the same behavior. Fig. 9, at the right, shows also a zoom window around the horizontal axis, it can be seen that, in general, the Whillier [9] model is very near the horizontal axis, immediately after are CPRG and Gueymard, then Liu and Jordan [10], Garg and Garg [11], and CPR which is the farthest (compared to the other first group). But CPRG and Gueymard are the best for March, September and October. Models from the second group have the worst (highest) value of NMBE%.

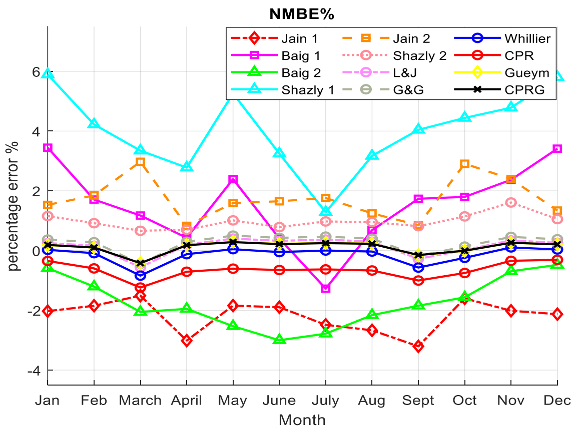

(a)

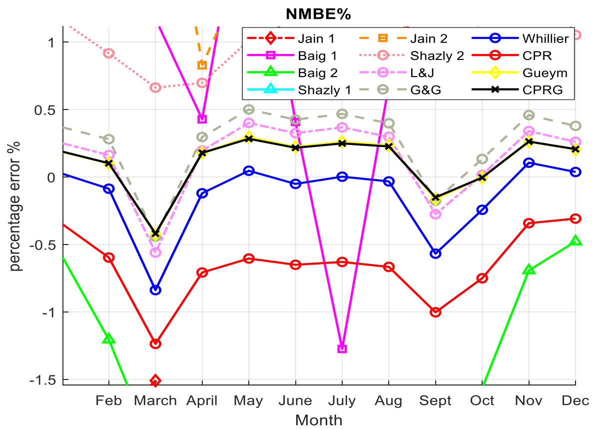

(b)

Fig. 9. Plot of NMBE% versus month: (a) general scope, (b) zoom window around horizontal axis.

The value of the NMBE% for the first group can be very low. Table 9 shows that the NMBE% value for Whillier model is 0.001% for winter season. This latter as a first approach is an indication of a very good estimate, but as it will be seen afterward, it is not a sufficient condition. Fig. 10 gives the plot of NMABE% and NRMSE%, the more the value is low towards zero, better the model is. Models on the second group are the best here, especially Baig 1, Shazly 1, and Baig 2. A set of best models can be built, this set includes the following models, respectively with a hierarchy from top to down; Baig 1, Shazly 1, Baig 2, CPRG, Gueymard and CPR. Fig. 10 shows that these six models are near each other. The other models have higher percentage errors than the best set, especially Whillier [9], Liu and Jordan [10], and Garg and Garg [11] are the worst. The minimum for NMABE% and NRMSE%, especially for the best set, is for the month of July. Figs. 9 and 10 seem to be in opposition, because the model that has the lowest NMBE% has the highest NMABE% and NRMSE%. The reason is that for NMBE%, the sum of underestimation can be canceled or balanced by the sum of overestimation, which is not possible for NMABE% and NRMSE% because of the sum of absolute value or the square.

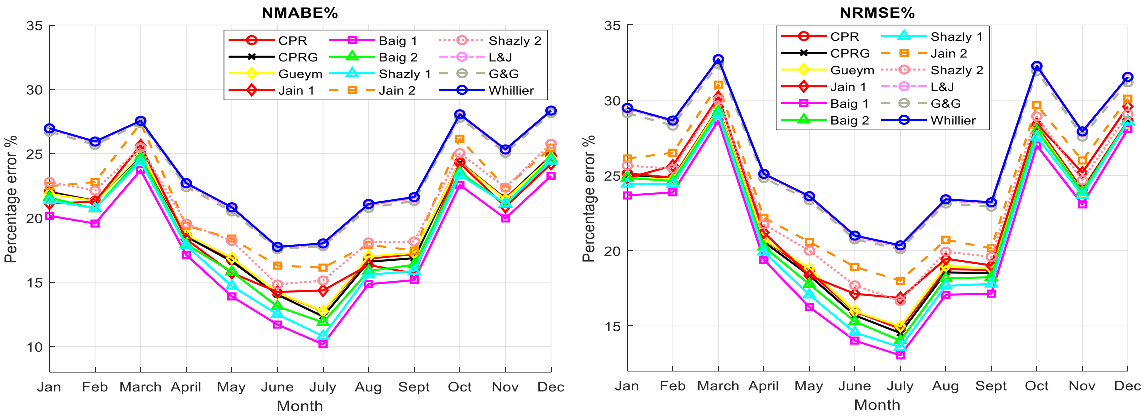

(a) (b)

Fig. 10. Plot of NMABE% and NRMSE% versus month: (a) NMABE%, (b) NRMSE%.

So, in order to finish the filling of the judgment matrix, the decision from this work is to give more importance to NMABE% and NRMSE% than NMBE% by factor 2. Fig. 11 gives the plot of RSE; the best model is whose with lowest RSE value towards to zero. The best models are in the second group model, especially Baig 1. Here also, a best set can be built with Baig 1, Baig 2, Shazly 1, CPR, CPRG, Gueymard, and Shazly 2. The other models have too much higher value than the best set. The minimum for the best set models is for the month of June. The maximum is for November.

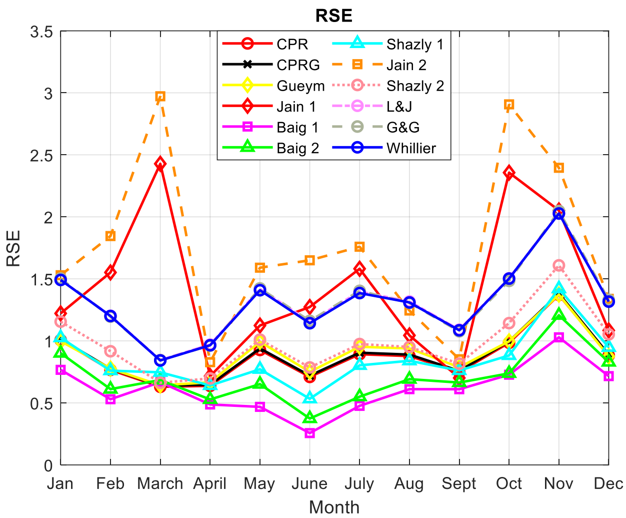

Fig. 11. Plot of RSE versus month.

Fig. 12 gives the plot for NSE and R. For these criteria the value of the best model should tend to 1. For NSE, the following models, in descending importance, form the best set: Baig 1, Shazly 1, Baig 2, CPRG, CPR and Gueymard. This ranking must not obscure that these models are near each other. The NSE value for the other models is clearly lower than the above mentioned set. For R, the values for all models are very near each other so the curves are like merging. The maximum is for the month of July.

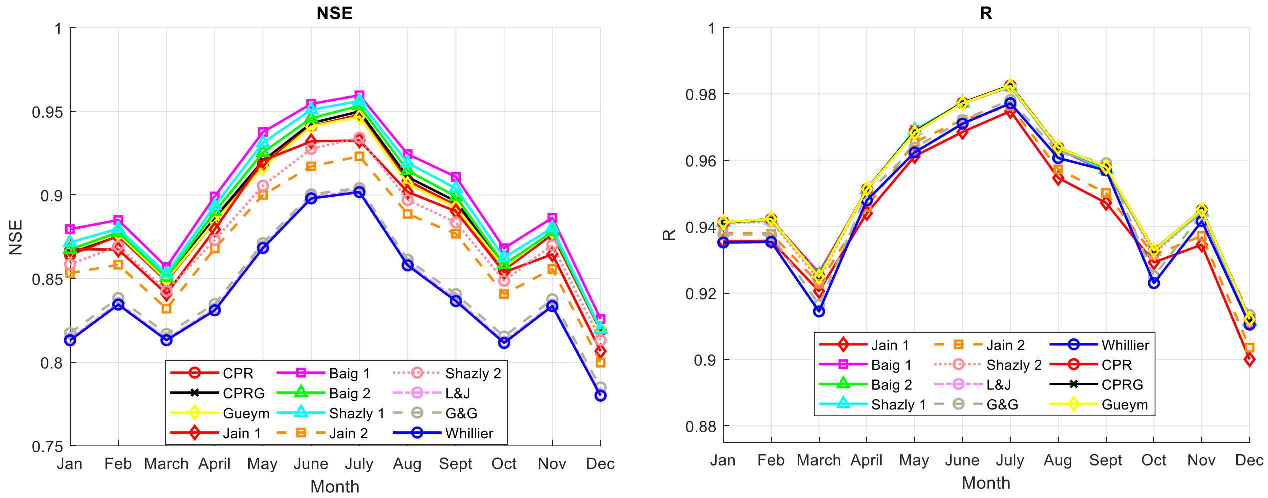

(a) (b)

Fig. 12. Plot of NSE and R versus month: (a) NSE, (b) R.

Finally Fig. 13, at the left, shows the plot of t-stat and at right a zoom window around the horizontal axis. The best models are those which t-stat value tends to zero or the point per point curve is getting closer to the horizontal axis (t-stat = 0). Like for NMBE%, the models from the first group are the best. In general, Whillier model has the lowest t-stat, and then, there are in decreasing order; CPRG, Gueymard, Liu and Jordan [10], Garg and Garg [11], and CPR. Models from second group have highest value of t-stat. CPRG and Gueymard are the best for the month of March, September, and October.

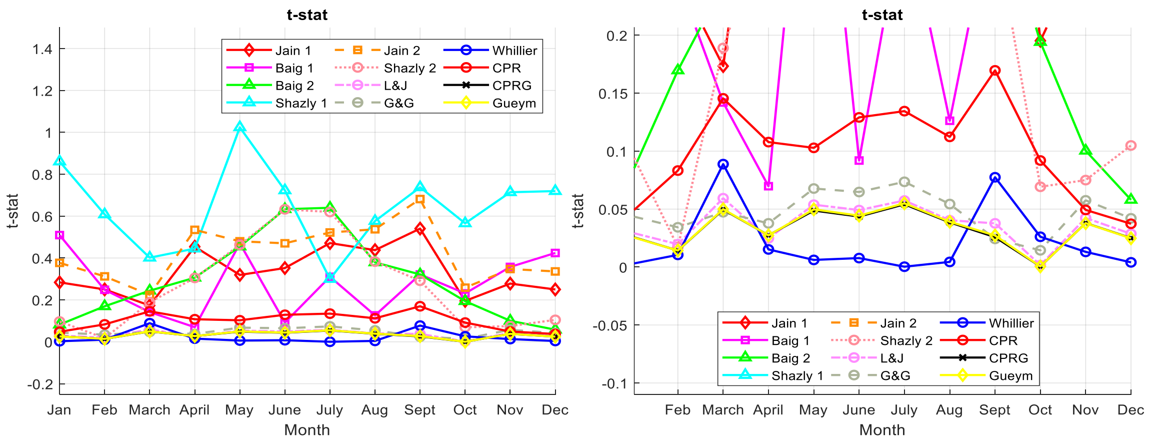

(a) (b)

Fig. 13. Plot of t-stat versus month: (a) general scope, (b) zoom around horizontal axis.

6.4. Results of the TOPSIS method

Table 11 gives the final judgment matrix for the subjective AHP weight, where the hierarchy between NMBE%, NMABE%, and NRMSE% was posed.

Table 11. Final Judgment Matrix

	NSE	R	RSE	NMBE%	NMABE%	NRMSE%	t-stat
NSE	1	2	3	3	3	3	5
R	1/2	1	2	3	3	3	5
RSE	1/3	1/2	1	2	3	3	5
NMBE%	1/3	1/3	1/2	1	1/2	1/2	5
NMABE%	1/3	1/3	1/3	2	1	1	5
NRMSE%	1/3	1/3	1/3	2	1	1	5
t-stat	1/5	1/5	1/5	1/5	1/5	1/5	1

After calculation, the subjective weights are in Table 12 with CR that is lower than 0.1.

Table 12. Subjective Weight and CR by AHP Method

NSE	R	RSE	NMBE	NMABE	NRMSE	t-stat	CR
0.295	0.221	0.168	0.082	0.101	0.101	0.031	0.062

Table 13 shows the objective entropy weight.

Table 13. Objective Entropy Weight

Entropy	NSE	R	RSE	NMBE(%]	NMABE(%)	NRMSE(%)	t-stat
Year	0.001	4.08E-06	0.018	0.490	0.004	0.004	0.483
Summer	0.0003	7.60E-6	0.096	0.451	0.004	0.002	0.447
Winter	0.0005	4.44E-06	0.034	0.480	0.007	0.007	0.471
Jan	0.0006	7.04E-06	0.034	0.476	0.006	0.004	0.480
Feb	0.0003	7.62E-06	0.084	0.455	0.005	0.003	0.452
March	0.0003	0.00002	0.296	0.348	0.003	0.002	0.351
April	0.0005	3.47E-06	0.029	0.485	0.006	0.005	0.475
May	0.0005	7.27E-06	0.070	0.446	0.010	0.010	0.463
June	0.0003	6.15E-06	0.116	0.426	0.010	0.010	0.438
July	0.0004	5.41E-06	0.084	0.441	0.020	0.014	0.440
Aug	0.0005	0.000005	0.037	0.477	0.009	0.007	0.469
Sept	0.0007	6.32E-06	0.024	0.484	0.009	0.007	0.474
Oct	0.0003	0.00001	0.112	0.443	0.003	0.002	0.440
Nov	0.0005	6.74E-06	0.049	0.472	0.005	0.004	0.470
Dec	0.0004	0.00001	0.033	0.481	0.003	0.002	0.481

By Table 13, for entropy way, NMBE% and t-stat have the highest weight. It means that these criteria have the highest dispersion data value. The CRITIC weights are in Table 14.

Table 14. Objective CRITIC Weight

CRITIC	NSE	R	RSE	NMBE(%]	NMABE(%)	NRMSE(%)	t-stat
Year	0.035	0.005	0.216	0.045	0.026	0.024	0.649
Summer	0.017	0.005	0.580	0.025	0.018	0.015	0.341
Winter	0.028	0.004	0.245	0.039	0.023	0.024	0.638
Jan	0.027	0.005	0.363	0.037	0.026	0.022	0.520
Feb	0.018	0.005	0.549	0.027	0.021	0.016	0.363
March	0.009	0.005	0.790	0.014	0.009	0.009	0.164
April	0.031	0.004	0.225	0.044	0.025	0.024	0.646
May	0.021	0.004	0.354	0.031	0.019	0.021	0.551
June	0.016	0.003	0.394	0.026	0.016	0.018	0.527
July	0.017	0.003	0.387	0.025	0.019	0.019	0.529
Aug	0.027	0.004	0.296	0.036	0.024	0.024	0.589
Sept	0.034	0.006	0.234	0.039	0.030	0.026	0.632
Oct	0.014	0.005	0.716	0.018	0.013	0.012	0.223
Nov	0.021	0.004	0.514	0.027	0.023	0.019	0.391
Dec	0.028	0.007	0.370	0.042	0.031	0.021	0.502

By Table 14, there are RSE and t-stat that have the highest weight when the correlation between criteria is also taken into account. Then, Table 15 gives the final weight of the seven criteria by the algorithm of Fig. 3.

Table 15. Final Weight

w	NSE	R	RSE	NMBE(%]	NMABE(%)	NRMSE(%)	t-stat
Year	0.235	0.176	0.136	0.078	0.081	0.081	0.213
Summer	0.207	0.156	0.193	0.073	0.071	0.071	0.228
Winter	0.234	0.176	0.139	0.076	0.081	0.081	0.214
Jan	0.231	0.173	0.141	0.078	0.080	0.079	0.218
Feb	0.212	0.159	0.179	0.074	0.073	0.073	0.229
March	0.208	0.156	0.350	0.062	0.072	0.072	0.079
April	0.234	0.176	0.137	0.078	0.081	0.080	0.214
May	0.228	0.171	0.149	0.074	0.078	0.078	0.221
June	0.220	0.165	0.166	0.071	0.076	0.076	0.227
July	0.224	0.169	0.156	0.072	0.078	0.077	0.224
Aug	0.233	0.175	0.140	0.076	0.080	0.080	0.216
Sept	0.235	0.176	0.137	0.077	0.081	0.081	0.213
Oct	0.195	0.146	0.257	0.069	0.067	0.067	0.199
Nov	0.223	0.168	0.155	0.076	0.077	0.077	0.225
Dec	0.230	0.173	0.141	0.080	0.079	0.079	0.218

The seven criteria can be divided in two classes. The first class that has the highest weight includes NSE, t-stat, RSE and R. The second that has the lowest weight contains NMABE%, NRMSE% and NMBE%. This result shows the integration of subjective and objective weight, because, t-stat is the last priority from subjective way but high priority by entropy and CRITIC, and at the end, t-stat is in the high weight class. NSE and R are lower priority by objective weight but high priority from subjective way, and they are in the highest weight class also at the end. RSE is high priority whether for subjective or CRITIC method. For NMABE%, and NRMSE%, they were always lower priority whether for objective or for subjective way. After getting the final weights for each criterion, the TOPSIS method was applied and Tables 16, 17, and 18 show the score and the rank of all models according to the fifteen averaging period. The criterion is the relative closeness *rcn* to the worst solution (NIM). The best model is the one whose *rcn* is nearest 1 (far away NIM).

Table 16. Score and Ranking for Annual, Summer, and Winter Averaging

Annual	*rcn*	Summer	*rcn*	Winter	*rcn*
CPRG	0.958	Gueymard	0.948	CPRG	0.920
Gueymard	0.954	CPRG	0.947	Gueymard	0.912
G&G	0.857	Shazly2	0.916	CPR	0.879
CPR	0.856	CPR	0.900	Whillier	0.838
Liu&Jordan	0.849	Whillier	0.859	Liu&Jordan	0.827
Kaplanis	0.849	Liu&Jordan	0.858	Kaplanis	0.827
Whillier	0.835	Kaplanis	0.858	G&G	0.826
Newell	0.791	G&G	0.853	Baig1	0.807
Shazly2	0.760	Newell	0.806	Newell	0.780
Baig2	0.739	Baig2	0.805	Baig2	0.657
Baig1	0.731	Baig1	0.778	Shazly2	0.639
Jain1	0.471	Jain1	0.638	Jain1	0.553
Shazly1	0.365	Jain2	0.547	Jain2	0.428
Jain2	0.338	Jain3	0.533	Jain3	0.420
Jain3	0.324	Shazly1	0.429	Shazly1	0.380
Baig4	0.211	Jain5	0.373	Jain5	0.291
Baig3	0.165	Baig4	0.360	Jain4	0.262
Jain5	0.146	Jain4	0.345	Baig4	0.207
Jain4	0.114	Baig3	0.320	Baig3	0.165

For seasonal averaging, CPRG is the best for the annual and winter averaging and in second position for the summer season. Gueymard model is the best for summer season and in second position for yearly and winter averaging.

Table 17. Score and Ranking from January to June

Jan	*rcn*	Feb	*rcn*	March	*rcn*	April	*rcn*	May	*rcn*	June	*rcn*
Gueym	0.947	CPRG	0.945	CPRG	0.992	CPRG	0.941	CPRG	0.886	Baig 1	0.938
CPRG	0.944	Gueym	0.945	Gueym	0.991	Baig 1	0.940	Gueym	0.875	CPRG	0.890
CPR	0.930	Shazly 2	0.915	Baig 1	0.955	Gueym	0.935	CPR	0.862	Gueym	0.883
Baig 2	0.906	CPR	0.897	CPR	0.954	CPR	0.884	Whillier	0.801	CPR	0.860
Shazly 2	0.869	Whillier	0.858	G & G	0.936	Whillier	0.840	Liu & J	0.789	Whillier	0.807
Whillier	0.863	Kaplanis	0.856	Liu & J	0.935	Liu & J	0.837	Kaplanis	0.789	Liu & J	0.798
Liu & J	0.857	Liu & J	0.856	Kaplanis	0.935	Kaplanis	0.837	G & G	0.785	Kaplanis	0.798
Kaplanis	0.857	G & G	0.853	Shazly 2	0.933	G & G	0.836	Newell	0.746	G & G	0.794
G & G	0.851	Baig 2	0.810	Whillier	0.933	Newell	0.788	Jain 1	0.679	Newell	0.757
Newell	0.803	Newell	0.797	Baig 2	0.909	Baig 2	0.682	Baig 1	0.602	Jain 1	0.655
Jain 1	0.672	Baig 1	0.725	Newell	0.896	Shazly 2	0.668	Baig 2	0.600	Baig 2	0.561
Jain 2	0.553	Jain 1	0.636	Shazly 1	0.843	Shazly 1	0.528	Shazly 2	0.562	Jain 2	0.537
Jain 3	0.536	Jain 2	0.540	Baig 4	0.752	Jain 1	0.509	Jain 2	0.500	Jain 3	0.535
Baig 1	0.458	Jain 3	0.525	Baig 3	0.733	Jain 2	0.410	Jain 3	0.496	Shazly 2	0.520
Jain 5	0.371	Shazly 1	0.376	Jain 1	0.510	Jain 3	0.401	Jain 5	0.402	Shazly 1	0.496
Jain 4	0.343	Jain 5	0.363	Jain 2	0.370	Jain 5	0.254	Jain 4	0.379	Jain 5	0.460
Baig 4	0.332	Baig 4	0.336	Jain 3	0.356	Jain 4	0.222	Baig 4	0.263	Jain 4	0.441
Baig 3	0.252	Jain 4	0.334	Jain 5	0.192	Baig 4	0.215	Shazly 1	0.245	Baig 4	0.310
Shazly 1	0.188	Baig 3	0.295	Jain 4	0.173	Baig 3	0.172	Baig 3	0.226	Baig 3	0.281

Table 18. Score and Ranking from July to December

July	*rcn*	Aug	*rcn*	Sept	*rcn*	Oct	*rcn*	Nov	*rcn*	Dec	*rcn*
CPRG	0.906	CPRG	0.923	CPRG	0.945	CPRG	0.945	Gueym	0.938	Gueym	0.953
Gueym	0.898	Gueym	0.911	Gueym	0.934	Gueym	0.945	CPRG	0.937	CPRG	0.951
CPR	0.869	Baig 1	0.881	CPR	0.846	CPR	0.887	CPR	0.929	CPR	0.940
Whillier	0.825	CPR	0.873	G & G	0.836	Shazly 2	0.885	Baig 2	0.882	Baig 2	0.922
Liu & J	0.814	Whillier	0.835	Kaplanis	0.830	G & G	0.848	Shazly 2	0.880	Whillier	0.871
Kaplanis	0.814	Liu & J	0.826	Liu & J	0.830	Liu & J	0.846	Whillier	0.855	Kaplanis	0.864
G & G	0.809	Kaplanis	0.826	Whillier	0.819	Kaplanis	0.846	Kaplanis	0.847	Liu & J	0.864
Baig 1	0.776	G & G	0.824	Newell	0.775	Whillier	0.841	Liu & J	0.847	G & G	0.856
Newell	0.773	Newell	0.783	Shazly 2	0.721	Baig 2	0.801	G & G	0.838	Shazly 2	0.843
Shazly 1	0.770	Baig 2	0.634	Baig 1	0.713	Newell	0.787	Newell	0.786	Newell	0.800
Jain 1	0.588	Shazly 2	0.613	Baig 2	0.708	Baig 1	0.768	Jain 1	0.619	Jain 1	0.656
Baig 2	0.548	Jain 1	0.557	Jain 1	0.498	Jain 1	0.613	Baig 1	0.572	Jain 2	0.528
Jain 2	0.538	Shazly 1	0.446	Jain 2	0.349	Shazly 1	0.510	Jain 2	0.514	Jain 3	0.508
Jain 3	0.535	Jain 2	0.445	Jain 3	0.338	Jain 2	0.493	Jain 3	0.495	Baig 1	0.458
Shazly 2	0.527	Jain 3	0.439	Shazly 1	0.329	Jain 3	0.479	Jain 5	0.304	Jain 5	0.305
Jain 5	0.460	Jain 5	0.320	Baig 4	0.217	Baig 4	0.477	Jain 4	0.271	Baig 4	0.297
Jain 4	0.441	Jain 4	0.294	Jain 5	0.180	Baig 3	0.439	Baig 4	0.266	Jain 4	0.270
Baig 4	0.263	Baig 4	0.205	Baig 3	0.174	Jain 5	0.328	Shazly 1	0.239	Baig 3	0.215
Baig 3	0.234	Baig 3	0.165	Jain 4	0.149	Jain 4	0.303	Baig 3	0.218	Shazly 1	0.181

So, CPRG is the best for eight months (February, March, April, May, July, August, September, and October). CPRG is also in a second position for four months (January, June, November, and December). It means that CPRG is the best for eight months and in second position for the four remaining months. As seen above, CPRG is the best for the annual and winter averaging and in second position for the summer season. So, for the present work, CPRG model is the best model to estimate the mean hourly radiation based on the daily value for Roche Plate, Cirque de Mafate. In second position is Gueymard, because it is the best for three months (January, November, and December) and the summer season. Then, Gueymard model is also in the second position for other seven months (February, March, May, July, August, September and October).

6.5. Performance of the CPRG model

Seen that CPRG model is the best among the nineteen models, the present section will focus on its performance. Fig. 14 gives a graphical comparison between the measured data and the calculated data from CPRG model, for the monthly mean hourly irradiation.

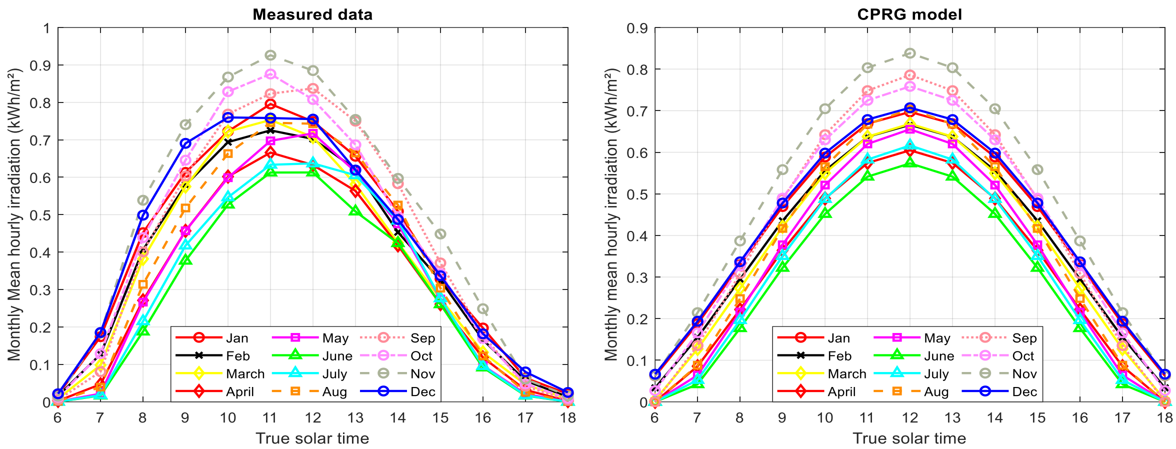

(a) (b)

Fig. 14. Monthly mean hourly irradiation from January to December: (a) measured, (b) CPRG model.

For the measured data, the maximum of the irradiation is at 11 h solar time for January, February, March, April, August, October, and November. This maximum is for noon solar time for May, June, July and September. For December, the maximum is at 10 h solar time. Seen that for CPRG model, the maximum is always at noon solar time, it is expected that the uncertainties or errors of the model will be lower for the months where the maximum is at noon solar time. Then, the monthly mean daily irradiation which is the sum of the monthly mean hourly irradiation during a representative day is calculated, the result is in Table 19.

Table 19. Measured and Estimated Monthly Mean Daily Irradiation in Decreasing Order

Month	Nov	Oct	Sept	Dec	Jan	Feb	March	Aug	May	April	July	June
Measured [kWh/m²]	6.28	5.49	5.45	5.40	5.30	4.88	4.71	4.67	4.24	4.07	3.95	3.64
CPRG [kWh/m²]	6.3	5.49	5.43	5.41	5.31	4.89	4.69	4.68	4.25	4.07	3.96	3.64
Relative difference in %	−0.26	0.00	0.33	−0.21	−0.19	−0.10	0.42	−0.16	−0.25	−0.06	−0.23	−0.20

Even there is a difference between measured and estimated irradiation value for each hour, the monthly mean daily value is practically the same because the relative difference is no more than 0.26% in absolute value. Fig 15. shows the same comparison but for annual, summer and winter average.

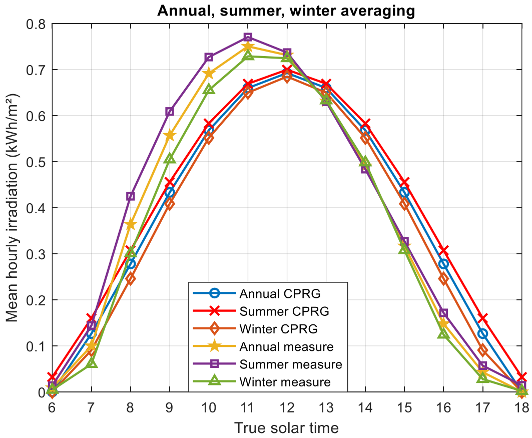

Fig. 15. Measured and calculated mean hourly irradiation for annual, summer, and winter averaging.

The maximum of irradiation for the measured data is at 11 a.m solar time. For the winter season, this maximum is still at 11 a.m but the value at noon solar time is very near the maximum. For CPRG model, the maximum is always at noon solar time. Due to the shift of the irradiation maximum hour, there is underestimation in the morning, and overestimation in the afternoon. Theoretically and practically, the annual value is the average of the summer and winter season. Table 20 shows the value of the measured and calculated mean daily irradiation for these three averaging periods.

Table 20. Measured and Estimated mean Daily Irradiation in Decreasing Order

Period	**Annual**	**Summer**	**Winter**
Measured [kWh/m^2]	4.831	5.109	4.571
CPRG [kWh/m^2]	4.823	5.114	4.577
Relative difference in %	0.18	−0.10	−0.13

With a relative difference not more than 0.2% in absolute value, here again; the CPRG model gives a very good estimate of the mean daily irradiation for the period of averaging. The next step now is to analyze the ability of the CPRG model to estimate the mean hourly irradiation from the daily value. Figs. 14. and 15. show the graphical difference between the measured and calculated value for the hourly irradiation. Table 21 gives the numerical value of the seven criteria for annual averaging, summer and winter season. To compare summer and winter season, the best value between them is highlighted in green.

Table 21. Statistical indicators for CPRG Model for the Annual, Summer and Winter Averaging

CPRG	**NSE**	**R**	**RSE**	**NMBE (%)**	**NMABE (%)**	**NRMSE (%)**	**t-stat**
Annual	0.863	0.938	0.672	0.006	19.18	20.92	0.001
Summer	0.872	0.939	0.7701	**0.100**	21.75	25.20	**0.014**
Winter	**0.909**	**0.962**	**0.7696**	0.277	**16.63**	**18.35**	0.048

The correlation coefficient R is between 0.938 and 0.962, which indicates a good fitting. The NMABE% is about 17% for winter and 22% for summer. The NRMSE% is 18% for winter and 25% for summer, with 21% for annual average. The NMBE% and t-stat are very low, 0.1% and 0.014 respectively for NMBE% and t-stat for summer season, that is another indicator of good fitting. By the highlighted values in Table 21, it can be assumed that the CPRG model is more efficient during austral winter than austral summer.

The next is to analyze the monthly performance of the CPRG model. Fig. 16(a) shows the curves of RSE and R for CPRG model for the twelve months, for these criteria more the value is near 1 more the model is better. The values of the correlation coefficient R are between 0.912 (December) and 0.983 (July), for NSE the values are between 0.82 (December) and 0.950 (July). For these indicators, the fitting is good. The look or behavior of the two curves is the same. The best performance period (highest value for R and NSE) for the CPRG model occurs between April to September with maximum in July, whereas less performance occurs during October to March. The lowest values are for March and December with minimum in December. The relative difference between December (worst efficiency) and July (best efficiency) is 7.22% for R and 14% for NSE.

Fig. 16 (b) gives the curves of NMABE% and NRMSE%, more the value is low towards zero, more the model is better. Here, the situation is exactly like the previous with NSE and R. The best performance period (lowest value for NMABE% and NRMSE%) is again during April to September, with the minimum value (highest performance) in July, 12.34% for NMABE% and 14.53% for NRMSE%. Conversely, the period of less efficiency is during October to March. The highest values (lowest efficiency) are for March and December. For NMABE%, the latter two months are very near each other, 24.9% for March and 24.8% for December. For NRMSE%, the maximum value is for March as 29.35% while it is 28.55% for December. The highest value for NMABE% and NRMSE% is around two times more than the lowest value. There is bigger gap between the highest and lowest value for NMABE% and NRMSE% than for NSE and R. The period of best performance during April to October with July for the maximum of efficiency is the reason why by Table 21, the CPRG model is more efficient during austral winter season than the austral summer season.

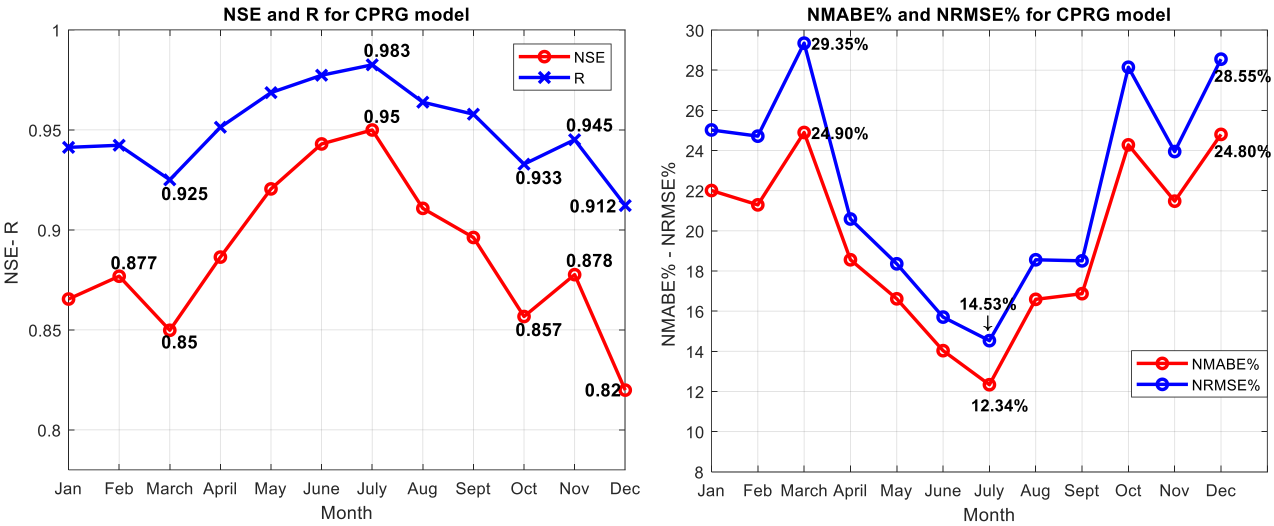

(a) (b)

Fig. 16. Monthly value for CPRG model: (a) NSE and R, (b)NMABE% and NRMSE%.

Fig 17(a). gives the plot of NMBE% and t-stat for the CPRG model. If NMBE% is negative, it means underestimation and conversely a positive value means overestimation. The model is better if NMBE% tends towards zero. For t-stat, which is always positive, the model is validated if the t-stat value is inferior to 2.7188 for twelve degrees of freedom. More the t-stat value tends towards zero, more the model is better.

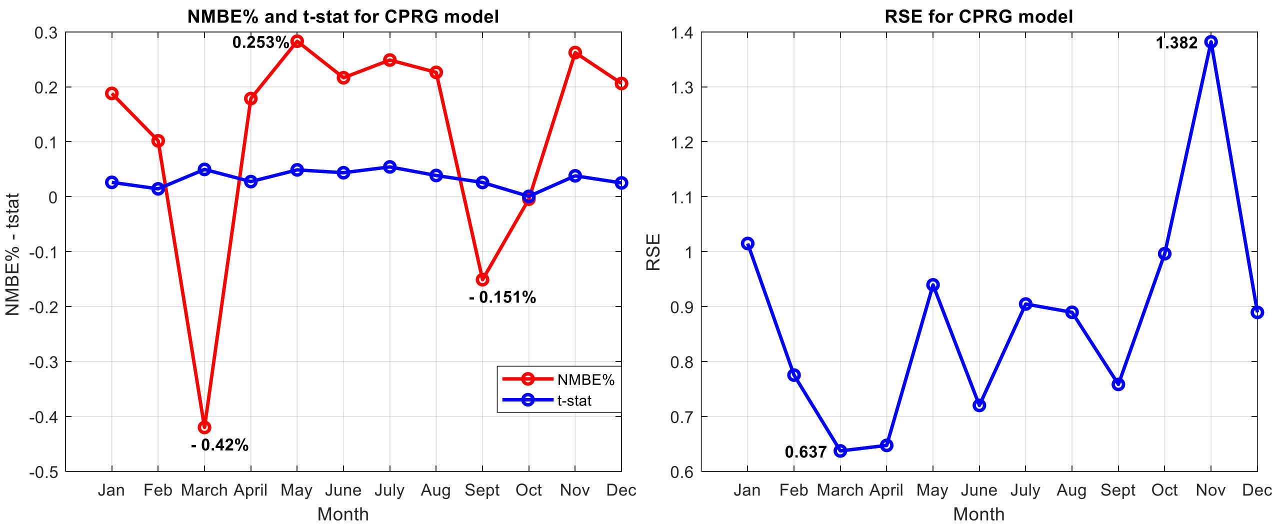

(a) (b)

Fig. 17. Monthly value for CPRG model: (a) NMBE% and t-stat, (b) RSE.

The t-stat value for all the twelve months does not exceed 0.1 for the CPRG model while the limit is 2.7188, so the model is well and largely valid. The minimum value is for October (t-stat = 0.001), and it is 0.014 for February. For NMBE%, there is underestimation in March (NMBE% = −0.42%) and September (NMBE% = −0.151%), and then there is overestimation for the other months with the exception of October where the NMBE% is −0.004% which can be practically considered like zero. The most negative value of NMBE% is −0.42% for March, and the most positive is 0.283% for May, these values are very small and practically can be considered like zero especially in front of the NMBE% values from second group's model.

Fig. 17(b) is for RSE, and more the value is low towards zero, more the model is better. The minimum value of RSE is for the month of March (RSE = 0.637) and the maximum is for month of November (RSE = 1.382). The ratio of highest RSE value and lowest RSE value is about 2.17.

7. Discussion

7.1. About the main features of the solar irradiation at the site

The weather at the Cirque of Mafate is very complex and special. Figs. 4–6 show that even the curve of the averaged hourly irradiation is bell-shaped for a representative day as expected, there is an asymmetry from solar noon time between morning and afternoon and the maximum is for 11 h not at noon solar time. The main reason comes from two things; the first is the cloud coverage and the second is the relief mask by the mountain wall on the west side. Figs. 7 and 8 show that the clearness index is high on the morning, i.e., it is a clear sky in the site with a maximum at 10 h and then the clearness index decreases as time passes, which means that there is a cloud coverage rising. At noon solar time, when the sun is at its maximum height, even it is still a clear sky for annual and winter averaging, the cloud coverage makes that the clearness index is already in its downward slope. For the summer average, at noon solar time, the clearness index is already below 0.6 which means the sky is partly cloudy. Seen that the highest relief mask is the wall mountain on the west side (Fig. 2), it is in the afternoon when the azimuth of the sun is on the west direction that its effect is predominant, significantly reducing the direct solar beam radiation from and around 16 h. This situation combined with whatever the cloud coverage makes that the clearness index is lower than 0.3 from 16 h. This reasoning explains the asymmetry and the maximum irradiation at 11 h. Theoretically, all models suppose that the maximum is at noon solar time, but the shift to 11 h means that there are underestimations in the morning and overestimations in the afternoon. For the future, the research of a new model that will be specific for the present site should take into account the clearness index and the solar relief mask by the surrounding topography.

7.2. About objective and subjective weight

Objective and subjective weight have all their advantages and disadvantages. It is the reason that they are used together. If the objective weight is automatic, discussion should be done for the subjective weight. The decision taken here is based on two points; the first is from previous paper [7] in the same field (estimating mean hourly radiation based on the daily value) where a primitive or rough hierarchy for the criteria, but without weight calculation or MCDM method, were done. The second is from analysis of the data; it was shown that for this study, NMBE% should have lower importance than NMABE% and or NRMSE%.

7.3. About the best model

The best model is CPRG followed by Gueymard according to the TOSPSIS result. Figs. 9–13 show that

CPRG and Gueymard are always in the best set of models, near the best model for each criterion, and for some months they are the best (months of March, September and October for NMBE% and t-stat). The models in second group, especially Baig 1, Shazly 1 and Jain 1 should be better because they are based on the knowledge of r_{12} that is the ratio of the hourly and daily irradiation at noon solar time, and their Gaussian distribution considers the random behavior of weather parameters. But, only Baig 1 and Baig 2 stand out among the other second group model. As a Gaussian distribution, these models suppose that the maximum is at noon solar time and there is symmetry between morning and afternoon, but as told above the real weather condition in the Cirque of Mafate is far from these conditions.

The analysis of the results and Figures show that Baig 1 is the best for some criteria for some months (NRMSE%, NMABE%, RSE and NSE) but at the end the TOPSIS method puts CPRG as the best, because Baig 1 and the entire second group's model fail too much on NMBE% and t-stat. The high dispersion value between the first group and second group for t-stat is the reason why t-stat has a high weight in the objective method as seen in Tables 13 and 14. Nevertheless, Baig 1 is the best for the month of June and in second position for April. But unfortunately, r_{12} is not a commonly available datum, so practically without it, Baig 1, Jain 1 and Shazly 1 are completely useless. By this latter, only Baig 2 can represent the second group model on this study, and its rank or score is far lower than CPRG and Gueymard.

So, for the Cirque of Mafate, the models from the first group are the good estimates. And between models in the first group, CPRG is the best, followed by Gueymard. This result is logical because the first group is based on the Whillier or Liu and Jordan [10] models and CPRG and Gueymard models are the best latter improvements.

7.4. Relationship between the performance of the best model and averaging period

The performance of the CPRG model depends on the averaging period. The model is more efficient, especially by NSE, R, NRMSE%, and NMABE% criteria during the period from April to September, with the maximal efficiency in July. And for the rest of the year (October to March), the performance is less with minimal efficiency in March and/or December. It is the reason why the model performs well for austral winter averaging than for austral summer averaging. For the months when the maximum irradiation hour is at noon solar time, the shift between the curve of measured and calculated data is reduced, so the errors are reduced and the model performs well. For the months when this maximum occurs at 11 h, the above-mentioned shift is emphasized and the model performs less. December is the month of minimal efficiency (highest errors and uncertainties) because the maximum irradiation hour is at 10 h, so the shift is maximal. All these specifications should be taken into account, in the future, for the research of a new model to estimate, for the present site, the mean hourly irradiation from the daily value.

8. Conclusion

The aim of this work is to study the main features of solar irradiation and to find among the existing the best model to estimate the mean hourly irradiation based on the daily value for the Cirque of Mafate. For the first target, it was found that following the meteorological and topographic parameters on the site, especially the cloud coverage, the rugged terrain and the relief mask around, the solar irradiation is very atypical with a maximum at 11 h solar time, and asymmetry between morning and afternoon because in general it is a clear sky in the morning and the afternoon is cloudy. The surrounding relief starts also to obscure the direct solar beam radiation from around 16 h. For the second target, all existing models in the literature as well as their variants were used, so nineteen models altogether. Seven statistics criteria were used to evaluate the performance of each model. The assessment was done by the principle of the Multi Criteria Decision Making, and especially the TOPSIS method where the best ideal solution and the worst solution are identified, then the best model is the one that is nearest the best solution or farthest the worst.

For TOPSIS, a hierarchy between the criteria reflected by the weight for each criterion must be established. Subjective and objective weights were used together. If the objective weight is automatic, the subjective weight depends on human knowledge and judgment. The experience from similar previous work and present data analyze are the base of the judgment matrix used to get the subjective weight. In the end, the results show that CPRG is the best model and Gueymard is in the second position.

The present work shows the problem of studying solar irradiation at a rugged terrain and relief in a high mountain place like the Cirque of Mafate. The atypical behavior of the solar irradiation at the present site means that future work should focus on the research of a new solar irradiation model that considers all meteorological, solar and topographic parameters.

Conflict of Interest

The authors declare no conflict of interest.

Author Contributions

Conceptualization, Tovondahiniriko Fanjirindratovo and Didier Calogine; methodology, Tovondahiniriko Fanjirindratovo, and Didier Calogine; software, Tovondahiniriko Fanjirindratovo; validation, Didier Calogine, Oanh Chau. and Olga Ramiarinjanahary.; formal analysis, Tovondahiniriko Fanjirindratovo, Didier Calogine, Oanh Chau; investigation, Tovondahiniriko Fanjirindratovo, and Didier Calogine; resources, Tovondahiniriko Fanjirindratovo, and Didier Calogine; data curation, Tovondahiniriko Fanjirindratovo; writing—original draft preparation, Tovondahiniriko Fanjirindratovo; writing—review and editing, Didier Calogine, Oanh Chau., and Olga Ramiarinjanahary; visualization, Tovondahiniriko Fanjirindratovo, and Didier Calogine; supervision, Didier Calogine, Oanh Chau., and Olga Ramiarinjanahary; project administration, Didier Calogine; funding acquisition, Didier Calogine All authors had approved the final version.

Funding

This study was made possible thanks to a cooperation between the University of Reunion Island and the University of Toliara, under the “Micro Reseau Mafate project” that is funded by the European Regional Development Fund, the Reunion Council, and the French Government.

Acknowledgment

The authors would like to express their many thanks to the “Service de Cooperation et d’Action Culturelle” of the French Embassy in Madagascar for financially supporting the travel and the stay of the first author at the PIMENT Laboratory for the purpose of writing the present paper, in the context of an “HDR stay” program.

References

[1] Calogine, D., Chau, O., & Lauret, P. (2019). A fractional derivative approach to modeling a smart grid-off cluster of houses in an isolated area. *Journal of Applied and Numerical Optimization, 1(3)*, 347–362.

[2] Fanjirindratovo, T., Calogine, D., Ramiarinjanahary, O., Chau, O., Francou, J., Dotti, S., Rasoavonjy, & P. (2023). Micro Reseau Mafate. Optimization of an isolated smart grid by real time management of user’s needs and available resources. *Poster Presentation during Solar Technologies & Hybrid Mini Grids to Improve Energy Access Conference*. 26–28 April 2023. Palma de Mallorca. Spain

[3] Abbezzot, C., Francou, J., & Calogine, D. (2022). Demand side management applied to a stand-alone microgrid. *International Journal of Smart Grid Clean Energy, 11(4),* 127–134.

[4] Francou, J., Calogine, D., Chau, O., Ramiarinjanahary, O., Fanjirindratovo, T., & Rasoavonjy, P. (2019).

Micro réseau mafate project, smart grid development by experimenting an off-grid microgrid, *Proceedings of the 11th High Energy Physics Madagascar International Conference* (HEPMAD19). Antananarivo, Madagascar.

[5] Calogine, D., Francou, J., Abbezzot, C., & Fanjirindratovo, T. (2023). Data in experimental stand-alone microgrid: Solar production, domestic loads, battery storage and meteorological series. *Data in Brief*, 51.

[6] Michalsky, J. J. (1988). The Astronomical Almanac's algorithm for approximate solar position (1950–2050). *Solar Energy, 40(3),* 227–235.

[7] de Miguel, A., Bilbao, J., Aguiar, R., Kambezidis, H., Negro, E. (2001). Diffuse solar irradiation model evaluation in the North Mediterranean belt area. *Solar. Energy*, *70,* 143–153.

[8] Yao, W., Li, Z., Xiu, T., Lu, Y., & Li, X. (2015). New decomposition models to estimate hourly global solar radiation from the daily value. *Solar Energy*, *120,* 87–99,

[9] Whillier, A. (1956). The determination of hourly values of total solar radiation from daily summations. *Arch. Met. Geoph. Biokl. B.*, *(7),* 197–204.

[10] Liu, B. Y. H., & Jordan, R. C. (1960). The interrelationship and characteristic distribution of direct, diffuse and total solar radiation. *Solar. Energy*, *4,* 1–19.

[11] Garg, H. P., Garg, S. N. (1987). Improved correlation of daily and hourly diffuse radiation with global radiation for Indian stations. *Solar Wind Technology, 4,* 113–126.

[12] Collares-Pereira, M., Rabl, A. (1979). The average distribution of solar radiation-correlation between diffuse and hemispherical and daily and hourly insolation values. *Solar Energy*, *22,* 155–164.

[13] Gueymard, C. (1986). Mean daily averages of beam radiation received by tilted surfaces as affected by the atmosphere. *Solar. Energy*, *37,* 261–267.

[14] Gueymard, C. (2000). Prediction and performance assessment of mean hourly global radiation. *Solar. Energy*, *68,* 285–303.

[15] Kaplanis, S. N. (2006). New methodologies to estimate the hourly global solar radiation: comparisons with existing models. *Renewable Energy, 31,* 781–790.

[16] Jain, P. C. (1984). Comparison of techniques for the estimation of daily global irradiation and a new technique for the estimation of global irradiation. *Solar Wind Technology, 1,* 123–134.

[17] Jain, P. C. (1988). Estimation of monthly average hourly global and diffuse irradiation. *Solar Wind Technology*, *5,* 7–14.

[18] Baig, A., Akhter, P., & Mufti, A. (1991). A novel approach to estimate the clear day global radiation. *Renewable Energy, 1,* 119–123.

[19] Shazly, S. M. E. (1996). Estimation of hourly and daily global solar radiation at clear days using an approach based on modified version of Gaussian distribution. *Advances in Atmospheric Sciences, 13(3),* 349–358.

[20] Newell, T. A. (1983). Simple models for hourly to daily radiation ratio correlations. *Sol. Energy, 31,* 339–342.

[21] Zhao, N., Zeng, X., & Han, S. (2013). Solar radiation estimation using sunshine hour and air pollution index in China. *Energy Conversion Management*, *76,* 846–851.

[22] Ulgen, K., & Hepbasli, A. (2009). Diffuse solar radiation estimation models for Turkey's big cities. *Energy Conversion Management, 50,* 149–156.

[23] Dutta, B., Dao, S. D., Martínez, L., & Goh, M. (2021). An evolutionary strategic weight manipulation approach for multi-attribute decision making: TOPSIS method. *International Journal of Approximate Reasoning*, *129,* 64–83.

[24] Mousavi-Nasab, S. H., & Sotoudeh-Anvari, A. (2017). A comprehensive MCDM-based approach using

TOPSIS, COPRAS and DEA as an auxiliary tool for material selection problems. *Materials & Design*, 121, 237–253.

[25] Das D., Sharma R. K., Saikia, P., & Rakshit D. (2021). An integrated entropy-based multi-attribute decision-making model for phase change material selection and passive thermal management. *Decision Analytics Journal*, *1,* 100011.

[26] Odu, G. O. (2019). Weighting methods for multi-criteria decision making technique. *Journal of Applied Sciences and Environmental Management, 23(8).*

[27] Dwivedi, P. P., & Sharma, D. K. (2023). Evaluation and ranking of battery electric vehicles by Shannon's entropy and TOPSIS methods. *Mathematics and Computers in Simulation*, *212,* 457–474.

[28] Agar, D. A., Hansen, P., Rudolfsson, M., & Blagojević, B. (2023). Combining behavioural TOPSIS and six multi-criteria weighting methods to rank biomass fuel pellets for energy use in Sweden. *Energy Reports*, *10,* 706–718.

[29] Diakoulaki, D., Mavrotas, G., & Papayannakis, L. (1995). Determining Objective Weights in Multiple Criteria Problems: The Critic Method. *Computer & Operation Research, 22,* 763–770.

[30] J. Yin, Du, X., Yuan, H., *et al*. (2021). TOPSIS power quality comprehensive assessment based on a combination weighting method. *Proceedings of the IEEE 5th Conference on Energy Internet and Energy System Integration (EI2)* (pp. 1303–1307). Taiyuan, China.

[31] Zhangzhen, L., Haifan, J., Jianlin, F., & Guofu, D. (2021). Combination weighting-based comprehensive evaluation for discrete workshop production plan. *Journal of System Simulation, 33(8),* 1856–1865.

[32] Ai, L., Liu, S., Ma, L., *et al*. (2019). A multi-attribute decision making method based on combination of subjective and objective weighting. *Proceedings of the 5th International Conference on Control, Automation and Robotics (ICCAR)* (pp. 576–580). Beijing, China.

[33] Wan Nik, W. B., Ibrahim, M. Z., Samo, K. B., & Muzathik, A. M. (2012). Monthly mean hourly global solar radiation estimation. *Solar Energy, 86,* 379–387.

[34] Ayvazoğluyüksel, Ö., & Filik, Ü. B. (2017). Estimation of monthly average hourly global solar radiation from the daily value in Çanakkae, Turkey. *Journal of Clean Energy Technologies, 5(5).*